Final Report

MINOR RESEARCH PROJECT

ENTITLED

“PHOTOCATALYTIC DEGRADATION OF DYES IN POLLUTED WATER”

Under CPE scheme of UGC for Faculty Enrichment

BY

Dr. Rupy Dhir

GENERAL SHIVDEV SINGH DIWAN GURBACHAN SINGH

KHALSA COLLEGE PATIALA

An Autonomous College

NAAC Accredited 'A' Grade

College with Potential for Excellence Status by UGC

ACKNOWLEDGEMENTS

First of all, I pay my gratitude to the Almighty for granting me an opportunity and strength to successfully accomplish this assignment.

My heartfelt gratitude and indebtedness goes to my husband, Dr. Khanesh Kumar, whose patience and love enabled me to complete this project work and who always stood besides me like a pillar in my difficult times. A sense of apology is due to my sweet daughter Pridhi and son Laveen who has probably missed many precious moments of motherly love and care. I would like to express my reverence and great admiration for my parents from whom I owe everything.

I am sincerely thankful to Dr. Dharminder Singh Ubha, Principal, G.S.S.D.G.S. Khalsa College, Patiala for commendable co-operation whenever sought and Dr. Ravinderjit Singh, Dean Research for providing me necessary facilities to pursue research work in the college.

It is privileged to extend special thanks to Dr. Narinder Singh, Associate Professor, Department of Chemistry, I.I.T. Ropar for allowing me to use his laboratory facilities.

I am also thankful to all the faculty members and non teaching staff of the Chemistry Department, who helped me a lot during this work. I would like to thank all research scholars and authors whose studies have been consulted and quoted in this study.

Finally, the financial assistance from UGC, India in form of research grant under CPE scheme of UGC for Faculty Enrichment is gratefully acknowledged.

Dr. Rupy Dhir

URKUND

Document Information

Analyzed document	ProjectReport11092020.docx (D78947697)
Submitted	9/11/2020 12:09:00 PM
Submitted by	
Submitter email	jaspreetissaj@gmail.com
Similarity	3%
Analysis address	jaspreetissaj.pununi@analysis.urkund.com

Sources included in the report

W	URL: https://www.sciencedirect.com/science/article/abs/pii/S0009261420302177 Fetched: 9/11/2020 12:10:00 PM	4
W	URL: https://shodhganga.inflibnet.ac.in/bitstream/10603/146370/18/18-publication.pdf Fetched: 11/19/2019 6:09:39 AM	2
SA	**Geetha. A.pdf** Document Geetha. A.pdf (D34209102)	1

CONTENTS

CHAPTER - 1
INTRODUCTION AND REVIEW OF LITERATURE

1.1 SEMICONDUCTOR NANOMATERIALS

Nano is derived from the Greek word "nanos" which means one billionth and denotes a factor of 10^{-9} or 0.000000001. The tendency to utilise individual atoms and molecules to produce nanostructured materials is known as nanotechnology. It is mainly related with the synthesis and utilization of molecules and devices mainly based on the size and shape of the materials. The particle size reduction of bulk solids to nanoregime causes a lot of changes in the physical and chemical properties. Semiconductor nanomaterials possess size dependent properties. When the size of the particle is reduced to the Bohr exciton radius, it exhibits the quantum confinement effect and large surface area to volume ratio. Due to the presence of quantum confinement effect and large surface to volume ratio nanomaterials exhibit strong size-dependent physical, chemical and optical properties with potential application in the field of optoelectronic, nanosensors, nanophosphors, nanophotocatalyst, photoconductor, bioimaging and laser materials.

1.2 WIDE BAND GAP SEMICONDUCTORS

Semiconductors are the materials which have band gap (energy difference between conduction and valence band) value higher than that of conductors but smaller than that insulators. This property makes the study of semiconductors an interesting field of research. Wide band gap of 3.4 eV as well as a large exciton binding energy of 60 meV makes ZnO a significant choice for researchers. ZnO is a n-type semiconductor due to its native doping caused by oxygen vacancies or zinc interstitials. But at room temperature oxygen vacancies can't provide free electrons and zinc interstitials are unstable. Hence doping of ZnO with various impurities is used to enhance its conducting properties.

1.3 PHOTOCATALYSTS

A catalyst is a substance which alters the rate of reaction without itself undergoing any physical and chemical change. The photocatalysts are the substances that chemically react with dyes in the presence of light and convert them into non toxic products by oxidation process. It can absorb light, produce electron hole pairs and bring chemical transformations. A photocatalyst should be stable, have wide band gap and be reusable. There are metal oxides like V_2O_3, Cr_2O_3, TiO_2, ZnO, SnO_3 etc. that possess the above mentioned characteristics and are capable of oxidizing organic substrates in the presence of light. Hence these metal oxides can be used as photocatalysts. Metal oxides show photocatalytic activity either by the generation of hydroxyl radicals upon oxidation of hydroxyl ions or by the generation of superoxide ions upon reduction of dioxygen. These hydroxyl radicals or superoxide ions degrade the harmful pollutants to harmless products.

1.4 MOTIVATION AND OBJECTIVES OF THE PRESENT WORK

Water pollution is one of the major environmental challenges, humankind is facing these days. The dyes which are widely used in textile, plastic, medicine and many other industries are the main cause of water pollution [1]. Azo dyes such as methyl orange constitutes about half of textile dyes [2]. The presence of these dyes in water sources contribute to toxicity, eutrophication and hinder the infiltration of sunlight, thus severely affect the growth of aquatic life [3] and causing long-term health effects [4]. Current methods including conventional sewage plant treatment [5] do not degrade harmful chemicals present in dyes and only insufficiently remove them from polluted water. An alternative and highly efficient technique for the degradation of dye is photocatalysis using semiconductor photocatalysts [6-9].

Comparing the photocatalytic activity of various semiconductor photocatalysts in aqueous media, zinc oxide (ZnO) is found to be on top

position [10, 11] and its photocatalytic activity can be further enhanced by moving from bulk to nano ZnO. [12]. It is because of large surface area of nanomaterials thus produces large number of active sites. The photocatalytic efficiency is further enhanced by adopting a number of strategies. Hybridization and supporting has greatly enhanced the photocatalytic efficiency of ZnO semiconductor. In a particular example photocatalytic efficiency of ZnO is enhanced by its hybridization of with graphite-like C_3N_4. Doping of ZnO nanomaterials further increases its photocatalytic efficiency towards the degradation of dyes. [13-23]. Literature study has revealed that doping of ZnO nanoparticles with rare earth metal atoms have significantly increased its photocatalytic efficiency towards the degradation of organic dyes in water [24-30]. Doping introduces another metal ions by substituting Zn ions from their original lattice points and produces traps photogenerated charge carriers which inturn lower the electron hole pair recombination rate, hence increases the photocatalytic efficiency.

During the present research work, emphasis has been given to synthesize and characterize efficient nano-photocatalysts for water purification and environmental cleaning. Gadolinium doped ZnO nanocrystals have been synthesized. The technique used for the synthesis of target nanocrystals is chemical co-precipitation method, a bottom up technique for the synthesis of nanoparticles. Synthesized nanomaterials are characterized by crystallographic, morphological, and various qualitative and quantitative techniques. Photo-catalytical behaviors of synthesized nanocrystals for the degradation of methyl orange dye in aqueous medium are also studied in detail.

In view of useful features of doped nanoparticles, synthesis and characterization of pure and doped nanocrystals to explore their photo-catalytic potential have been planned that include following objectives:

1. To synthesize pure and Gd doped ZnO semiconductor nanomaterials.
2. To study crystallographic and morphological characteristics of synthesized semiconductor nanomaterials.
3. To investigate photocatalytic degradation of methyl orange dye in the presence of synthesized semiconductor nanomaterials.

CHAPTER - 2
EXPERIMENTAL PROCEDURE

2.1 MATERIALS

Gadolinium (III) nitrate hexahydrate (99.9%) was purchased from Sigma Aldrich. Co, 3050, St.Louis, MO, USA, Zinc acetate, sodium hydroxide, polyvinyl pyrrolidone and methyl orange were of analytical reagent grade and used without further purification. All solutions used in the experiments were prepared by using triply distilled deionised water.

2.2 Synthesis of $Zn_{1-x}Gd_xO$ nanoparticles

Pure and gadolinium doped ZnO nanoparticles ($Zn_{1-x}Gd_xO$, $.00001 \leq x \leq 0.1$) were prepared using bottom up wet chemical co-precipitation technique in the presence of polyvinyl pyrrolidone (PVP) as a capping agent. Synthesis was carried out under ambient conditions. In the typical synthetic procedure, stoichiometric proportion of 0.5 M zinc acetate was taken in a titration flask followed by drop wise addition of gadolinium nitrate solution. After stirring the mixture for 1 hour, 8 ml. of 2% PVP was added and then 0.5 M sodium hydroxide solution was added drop wise with continuous stirring. Resulting white precipitates were filtered, thoroughly washed and then dried in hot air oven at 150°C temperature for one hour followed by crushing using mortar and pestle to obtain nanoparticles in fine powder form. Table 1 listed the amount of various precursors solution used for preparation of nanoparticles.

Sample Details $Zn_{1-x}Gd_xO$	**Amounts of precursors used in sample preparation**		
	Volume of 0.5 M $Zn(OCOCH_3)_2$ solution (ml)	Volume of 0.5 M NaOH solution (ml)	Volume of $Gd(NO_3)_3.6H_2O$ (M) solution (ml)
$x = 0.1$	45	50	1.04 (1 M)
$x = 0.01$	49.5	25	1.04 (0.1 M)
$x = 0.001$	49.95	25	1.04 (0.01 M)
$x = 0.0001$	49.995	25	1.04 (0.001 M)
$x = 0.00001$	49.9995	25	1.04 (0.0001 M)
$x = 0.0$	50	25	----

Table 1: Amount of precursors used in sample preparation

Equation (1) and (2) represents the stepwise formation of ZnO nanoparticles.

$$Zn(CH_3COO)_2(aq.) + 2NaOH(aq.) \xrightarrow{PVP} Zn(OH)_2(s) + 2CH_3COONa(aq.) \quad (1)$$

$$Zn(OH)_2(s) \xrightarrow{Heat} ZnO + H_2O \quad (2)$$

2.3 CHARACTERIZATION

The above prepared Gadolinium doped Zinc oxide nanoparticles have been characterized using various spectroscopic techniques namely X-ray diffraction, Field Emission Scanning Electron Microscopy, Fourier Transform infrared spectroscopy and energy dispersive x-ray fluorescence techniques. X-ray diffraction spectrum is obtained from powder X-ray diffraction (PAN-Analytic) setup using 3050/60 goniometer. The 2θ range selected for X- ray diffraction scans

was 20–80°.Cu K X-ray radiation with wavelength of 1.5406 Å at 40 mA–45 kV generator setting were used keeping step size 0.001 for the powder samples. For average particle size determination, an accelerating voltage of five thousand volts with magnification of 70000 were set using Hitachi (SU8000) FE scanning electron microscope and FE scanning electron microscopic micrographs were taken. The energy dispersive x-ray fluorescence technique is used to confirm the presence of various elements along with their composition in synthesized nanomaterials. EDXRF spectrometer having an excitation source of Mo anode X-ray tube (PAN-Analytic) and LEGe (Canberra made, FWHM = 150 eV at 5.89 keV) as photon detector is used to record spectra of the Gd doped ZnO nanomaterials. Fourier Transform Infrared studies were performed using Bruker alfa Fourier Transform Infrared spectrometer.

2.4 PHOTOCATALYTIC BEHAVIOUR

The photocatalytic behaviour of pure ZnO and Gd doped ZnO nanomaterials were studied under UV light exposure for the degradation of methyl orange dye in aqueous medium using UV-photoreactor equipped with one 160W UV-bulb which is about 10 cm above reaction mixture. Reaction mixture was prepared in a glass reactor with surface area 50 cm^2 by mixing 100 mg nanopowder in 250 ml of 16 ppm methyl orange dye solution and was used for photocatalytic studies. Very first the above solution was stirred in the absence of UV light in dark for one hour. It was resulted in the adsorption of dye atoms on the surface of nanoparticles. The solution was then exposed to the ultraviolet-radiation.5 ml of suspension solution was taken out and centrifuged at fixed time intervals. After centrifugation, the supernatant was analyzed using the ultraviolet–visible spectrophotometer. The concentration of dye was measured from the optical absorption values at a certain wavelength. The equation (3) represents the degradation efficiency (ε) of dye

$$\epsilon = \frac{Co - C}{Co} \times 100 \qquad (3)$$

whereas C_o and C represent the initial concentration of the dye the concentration after UV irradiation respectively. Furthermore, the photocatalytic degradation of methyl orange dye in the presence of synthesized nanoparticles follows pseudo-first-order kinetic equation (4) in accordance to the Langmuir–Hinshelwood kinetics model [24].

$$ln\frac{Co}{C} = \kappa t \qquad (4)$$

Where κ is the rate constant, C_o is the initial methyl orange concentration at time t = 0 and C is methyl orange concentration in aqueous solution at time t.

CHAPTER - 3
RESULTS AND DISCUSSION

3.1 CRYSTALLOGRAPHIC CHARACTERIZATION

Figure 1 represents the XRD patterns of all the synthesized pure and gadolinium doped ZnO nanoparticles ($Zn_{1-x}Gd_xO$, $.00001 \leq x \leq 0.1$). The successful synthesis, crystalline nature and hexagonal wurtzite structure of ZnO nanoparticles is confirmed from various sharp peaks in XRD graph observed at 2θ of 31.76°, 34.39, 36.22, 47.52, 56.54, 62.81, and 67.84 correspond to lattice planes (100), (002), (101), (102), (110), (103) and (112) respectively as reported in JCPDS file no. 05-0664 [32]. The lattice parameters 'a' and 'c' identified by JCPDS for hexagonal wurtzite ZnO are 3.2498 Å and 5.2066 Å respectively. Any diffraction peak related to impurity phase is not detected which indicates the successful substitution of Gd^{3+} ions into Zn^{2+} sites without disturbing wurtzite crystal structure of ZnO.

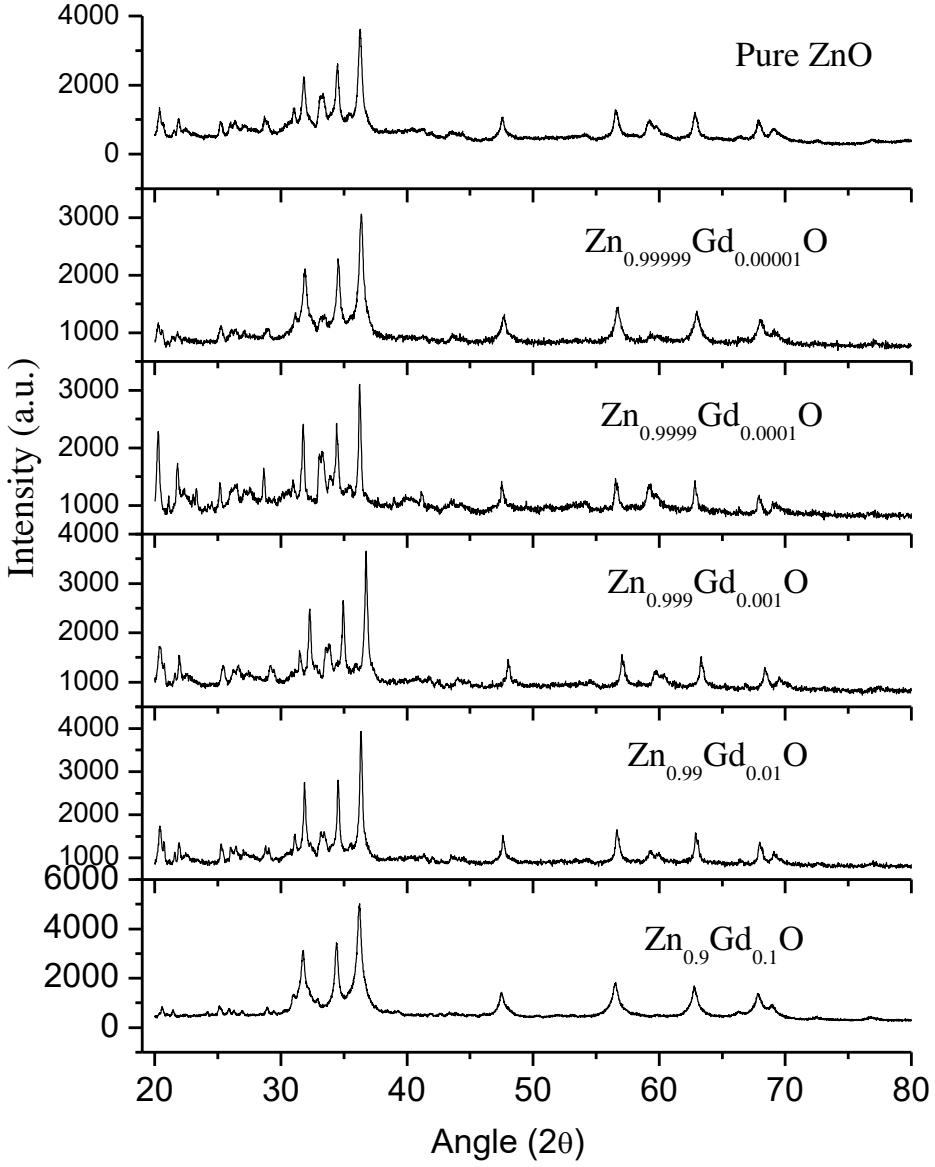

Fig. 1: X- ray diffraction spectra of PVP capped ZnO and $Zn_{1-x}Gd_xO$ ($0.00001 \leq x \leq 0.1$) nanoparticles Angle (2θ) ranges from 20 to 80.

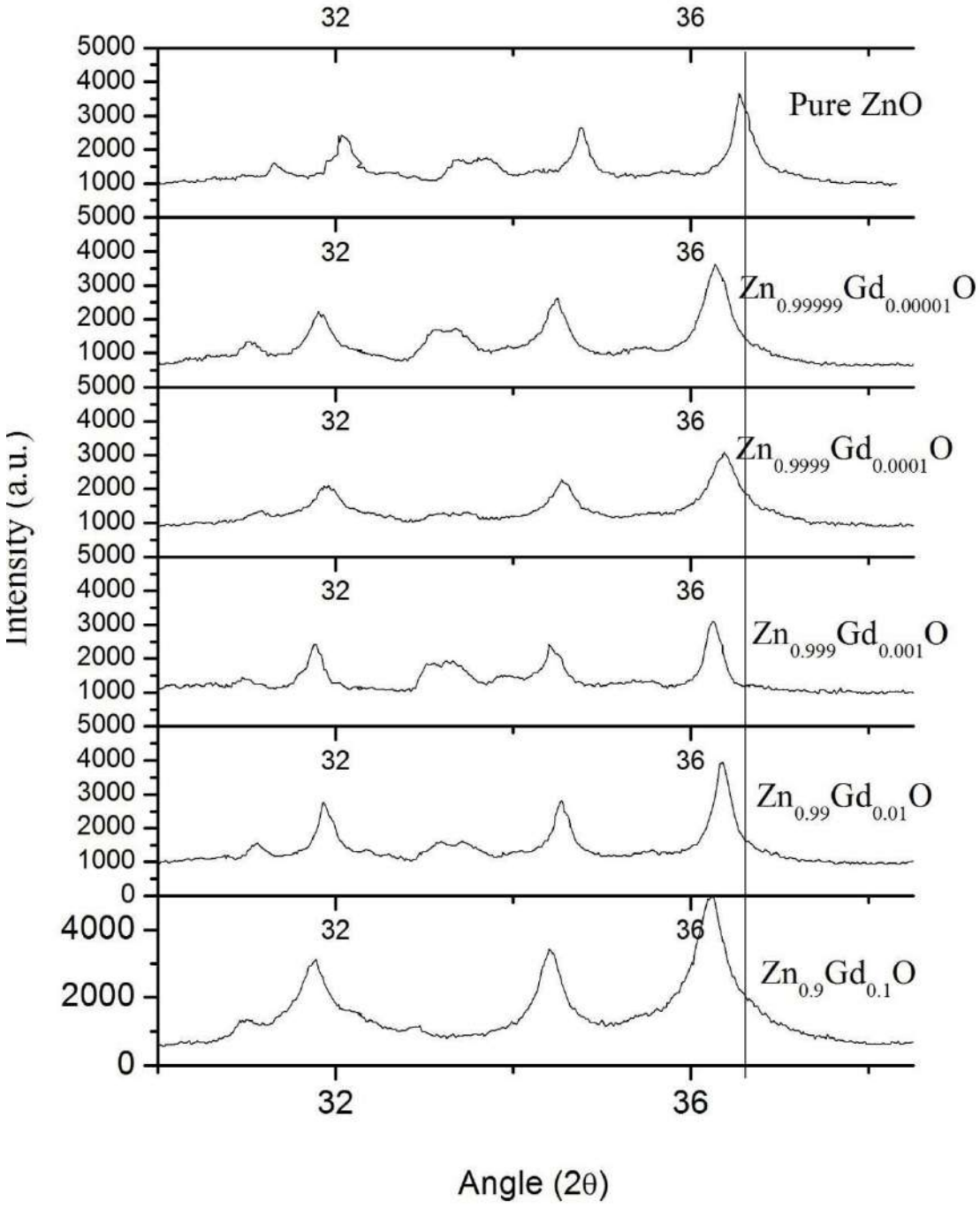

Fig. 2: X- ray diffraction spectra of PVP capped ZnO and $Zn_{1-x}Gd_xO$ ($0.00001 \leq x \leq 0.1$) nanoparticles Angle (2θ) ranges from 30 to 38.

The shifting of peaks shown in Figure 2 indicates the substitution of Gd in the crystalline ZnO structure. This is due to the expansion of ZnO lattice upon doping with Gadolinium as the ionic radii of Gd^{3+} (0.94 Å) is larger than that of Zn^{2+} (0.74 Å).

Scherrer'r formula [33] equation (5), by estimating full width at half maximum (FWHM) of sharp peak (101), was used to calculate the average crystalline size of the prepared nanoparticles .

$$D = \frac{0.89\,\lambda}{\beta \cos\theta} \qquad (5)$$

Where λ represents the wavelength of Cu K α radiation, β represents the diffraction peak's full width half maxima, and θ is the Bragg peak angle. Table 2 presents the crystalline sizes of synthesized nanoparticles at most intense crystallographic plane [110].

S. No.	**SAMPLE DETAILS** $Zn_{1-x}Gd_xO$	**AVERAGE CRYSTALLINE SIZE** (nm)
1..	$x = 0.1$	11.49
2.	$x = 0.01$	37.94
3.	$x = 0.001$	41.05
4.	$x = 0.0001$	52.67
5.	$x = 0.00001$	20.38
6	$x = 0.0$	18.62

TABLE 2: Estimated crystalline size from XRD data

3.2 FOURIER TRANSFORM INFRARED (FTIR) SPECTROSCOPIC STUDIES

Figure 3 represents FTIR spectra of synthesized nanoparticles. A peak at 3471 is assigned to O-H stretching where as other peak at 1396 $cm^{-1}$is assigned to O-H deformation which is attributed to water adsorption on the metal surface. Due to inter-atomic vibrations, metal oxides generally exhibit absorption bands in fingerprint region i.e. below 1000 cm^{-1}. The peak at 668 is corresponded to Zn-O stretching vibration, which is in accordance with literature values [34]. Various absorption peaks between 900 and 2900 cm^{-1} are also recorded in all samples. Absorption peaks around 900–1020 cm^{-1}, 1300-1600 cm^{-1} and 2850-2950 cm^{-1} are assigned to C–C stretching mode, C–O stretching modes (symmetric and asymmetric) and C–H bond of the acetate group respectively. The above observation and discussion indicates the presence of hydroxy and acetate groups on the surface of pure and Gd-doped ZnO nanoparticles.

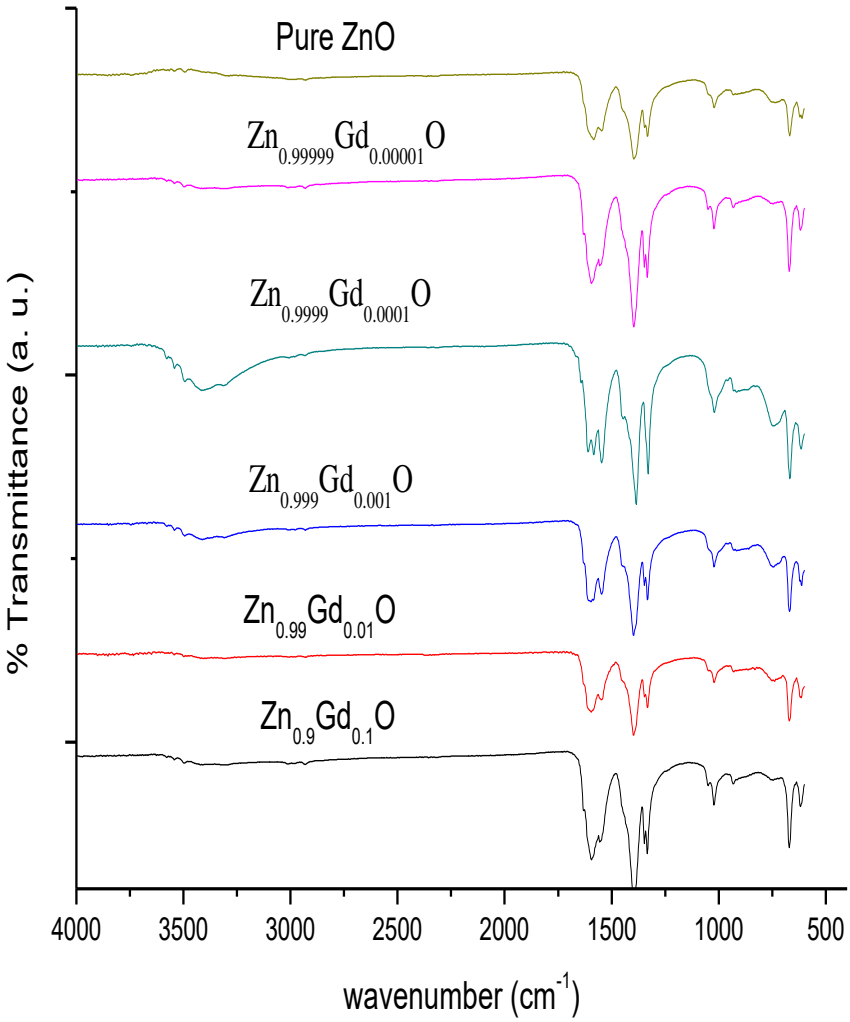

Fig. 3: Fourier Transform Infrared spectra of polyvinyl pyrrolidone capped $Zn_{1-x}Gd_xO$ (x = 0, 0.000001, 0.00001, 0.0001, 0.001, 0.01 and 0.1) nanocrystals.

3.3 ENERGY DISPERSIVE X-RAY FLUORESCENCE (EDXRF) STUDIES

Figures 4a-4d represent the chemical compositions of the prepared pure and gadolinium doped ZnO nanoparticles ($Zn_{1-x}Gd_xO$, $.001 \leq x \leq 0.1$) measured by EDS spectra. From the spectra 3a-3c, the presence of Zn, O and Gd is confirmed in Gd doped ZnO NPs whereas the spectrum 3d of pure ZnO NPs confirmed the presence of only zinc and oxygen ions. The obtained EDS result confirms the doping of ZnO matrix with Gd. The percentage amount of Gd calculated from EDS studies in $Zn_{1-x}Gd_xO$ samples is 1.02, 0.18 and 0.05 against theoretical value of 1, 0.1 and 0.01 for x = 0.01, 0.001 and 0.0001 respectively are shown in table 3. The experimental values are in good agreement with the calculated values.

S. No.	SAMPLE DETAILS $Zn_{1-x}Gd_xO$	Percentage amount of Gadolinium present in ZnO	
		Amount of Gd added	Experimental value
1.	$x = 0.01$	1	1.02
2.	$x = 0.001$	0.1	0.18
3.	$x = 0.0001$	0.01	0.05

Table 3: Percentage amount of Gd concentration in synthesized nanoparticles using EDXRF technique.

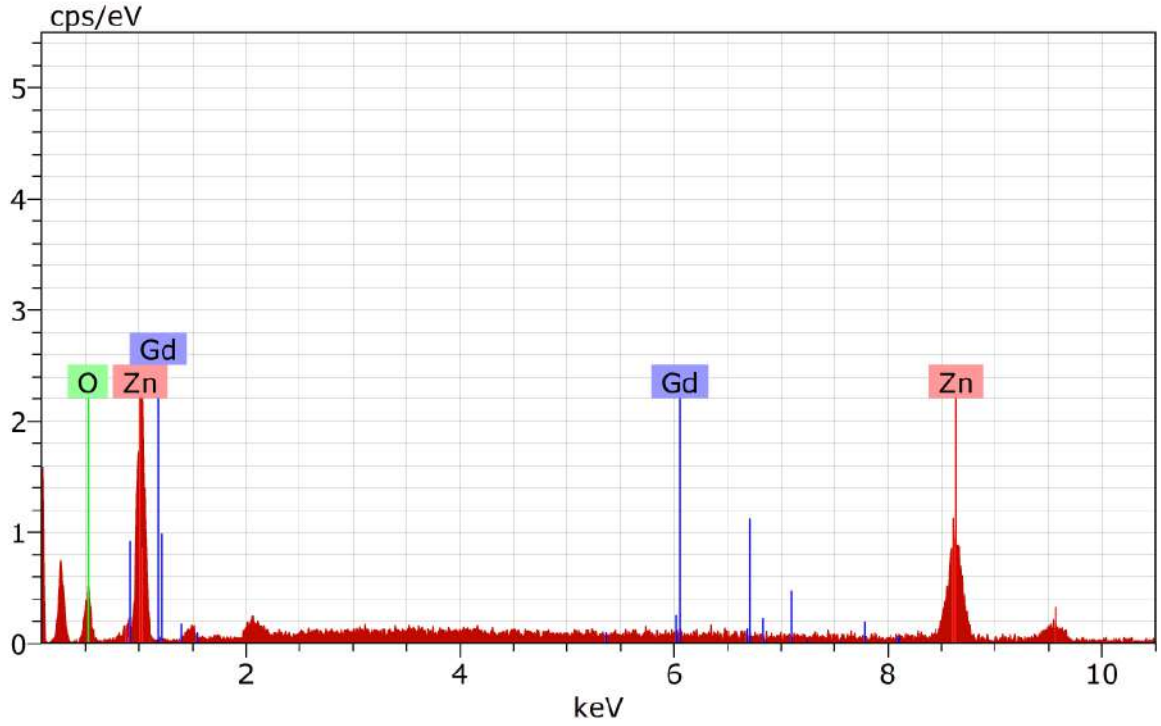

FIGURE 4a

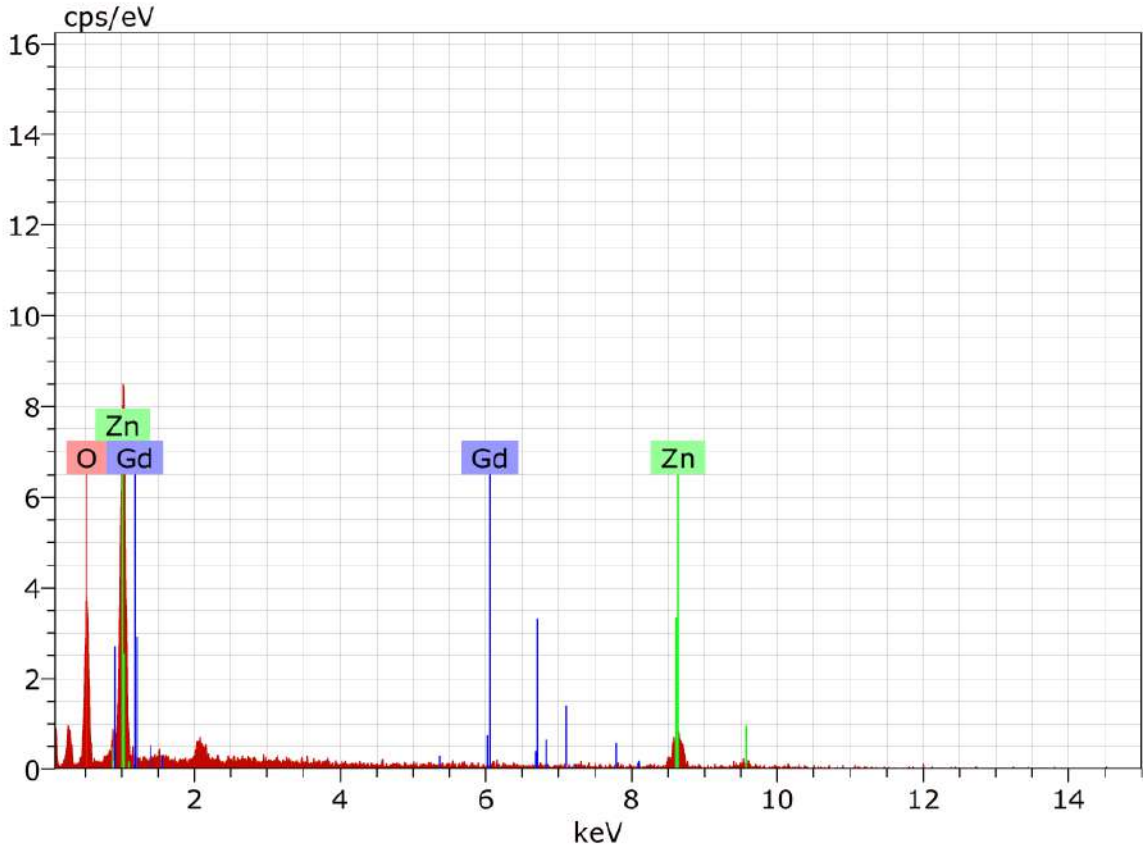

FIGURE 4b

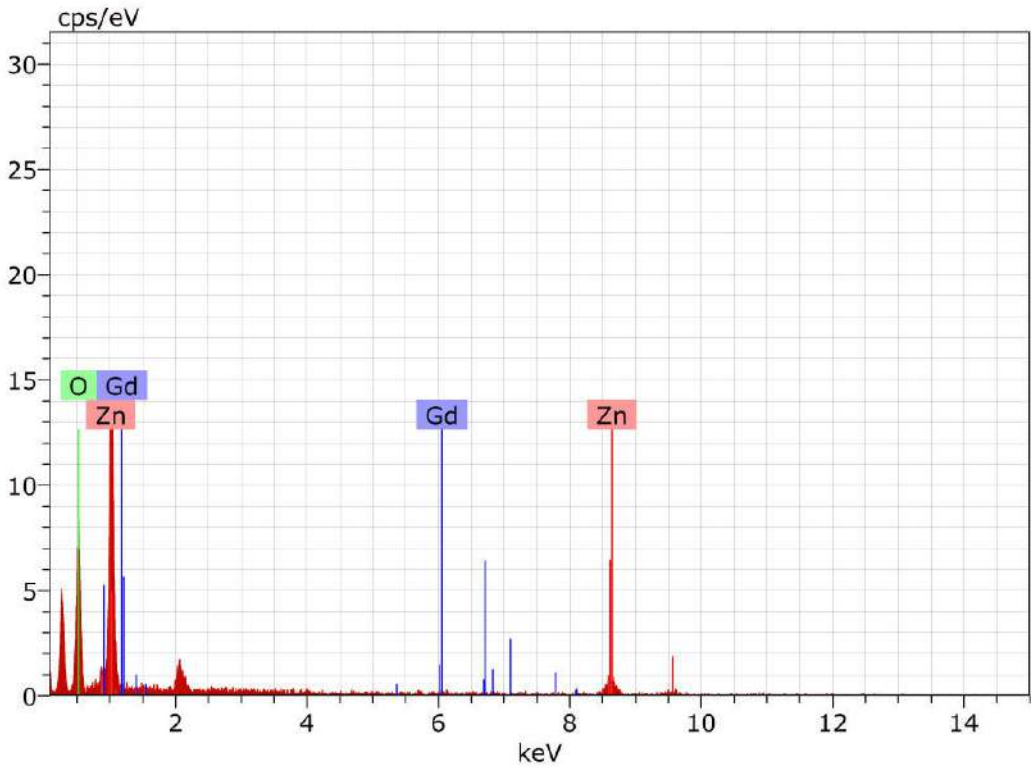

FIGURE 4c

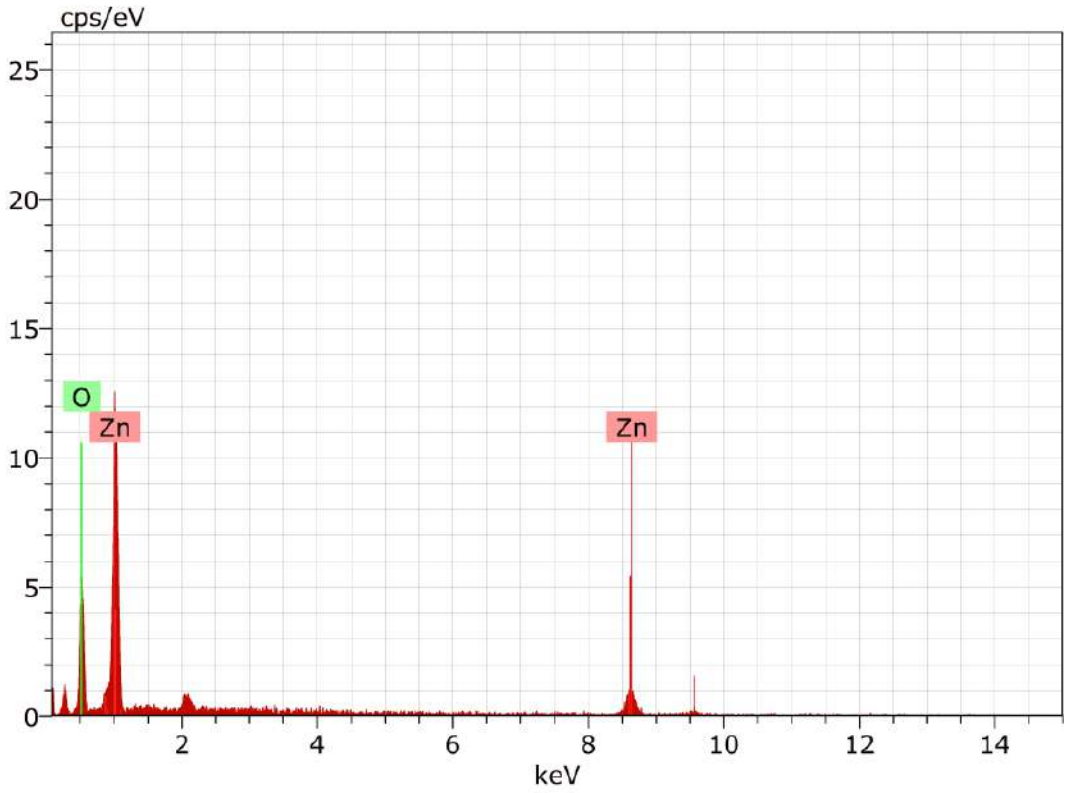

FIGURE 4d

Fig. 4: Energy dispersive x-ray fluorescence spectra of $Zn_{1-x}Gd_xO$ nanocrystals. (a) x=0.01, (b) x=0.001, (c) x=0.0001, (d) x=0.

3.4 FE SCANNING ELECTRON MICROSCOPIC STUDIES

The surface morphology of the PVP capped pure and Gd-doped ZnO nanoparticles were examined with FE scanning electron microscope. FE-SEM micrographs of $Zn_{0.9}Gd_{0.1}O$ Figure 5a, $Zn_{0.99}Gd_{0.01}O$ Figure 5b and pure ZnO Figure 5c nanoparticles show spherical clusters of particles. However, the doping with gadolinium results in a decrease in size of clusters.

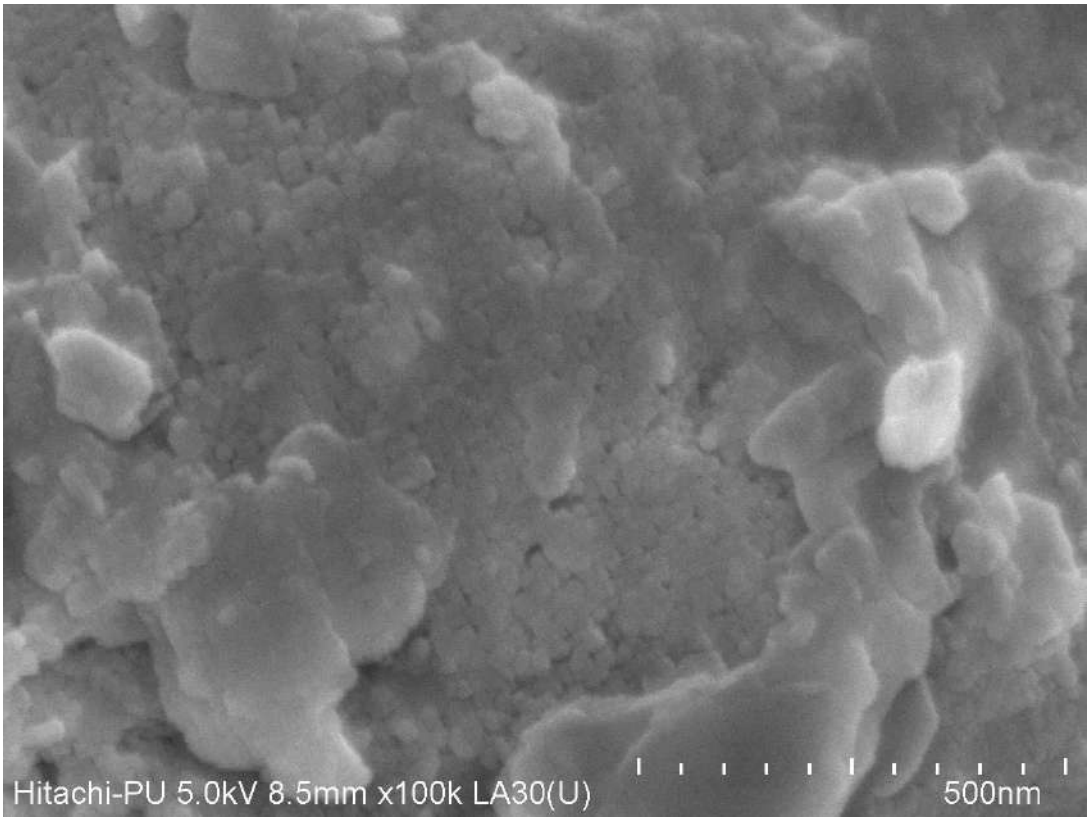

FIGURE 5a

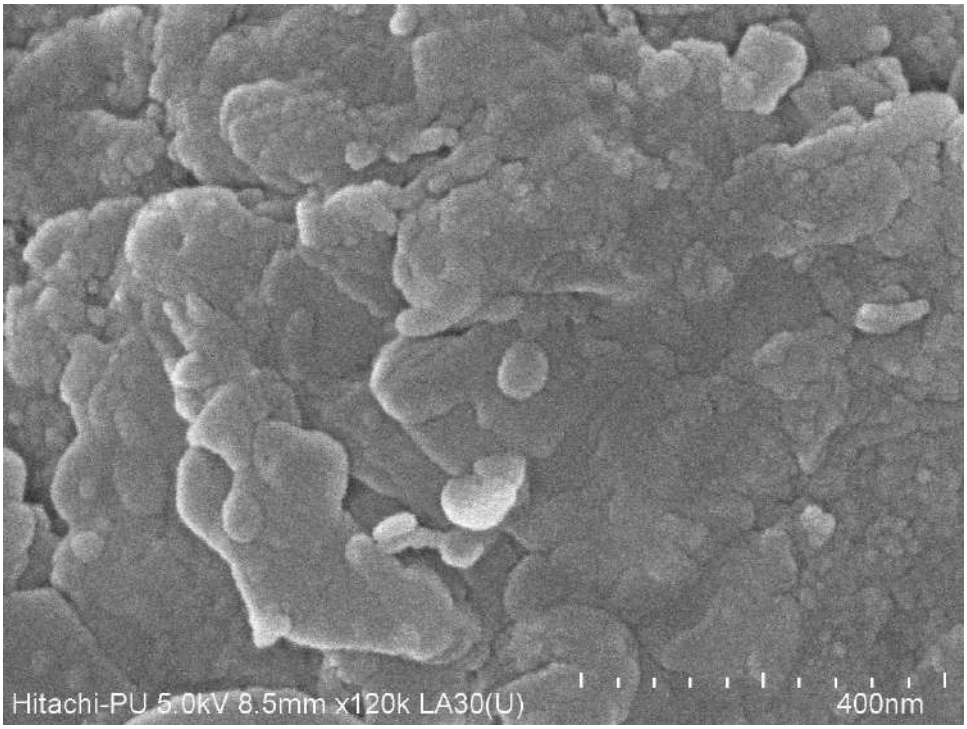

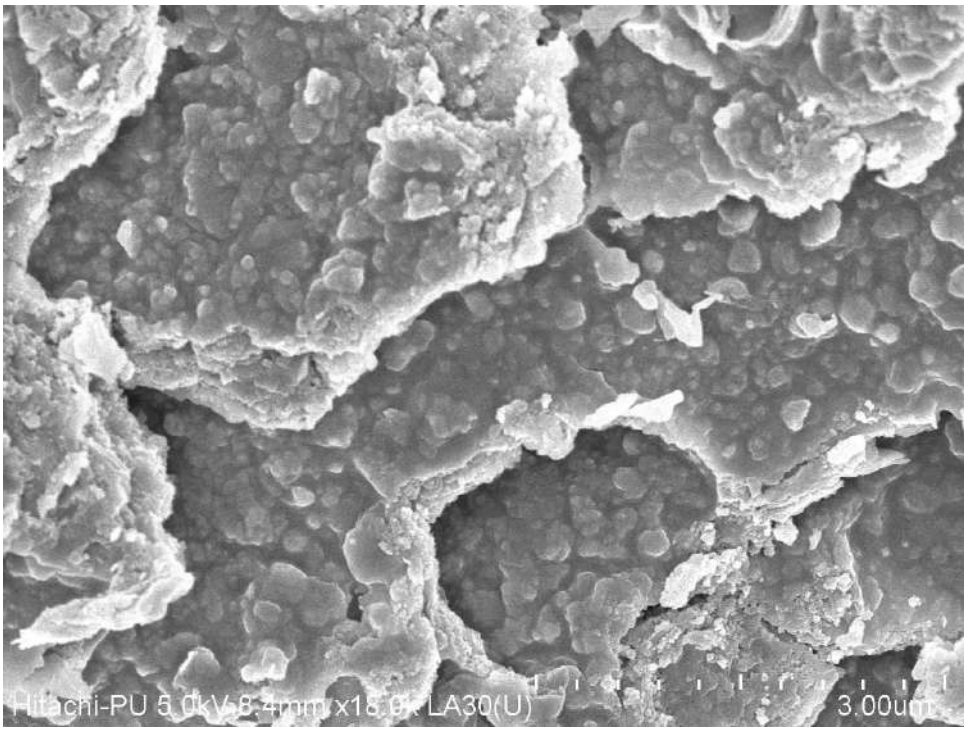

FIGURE 5b

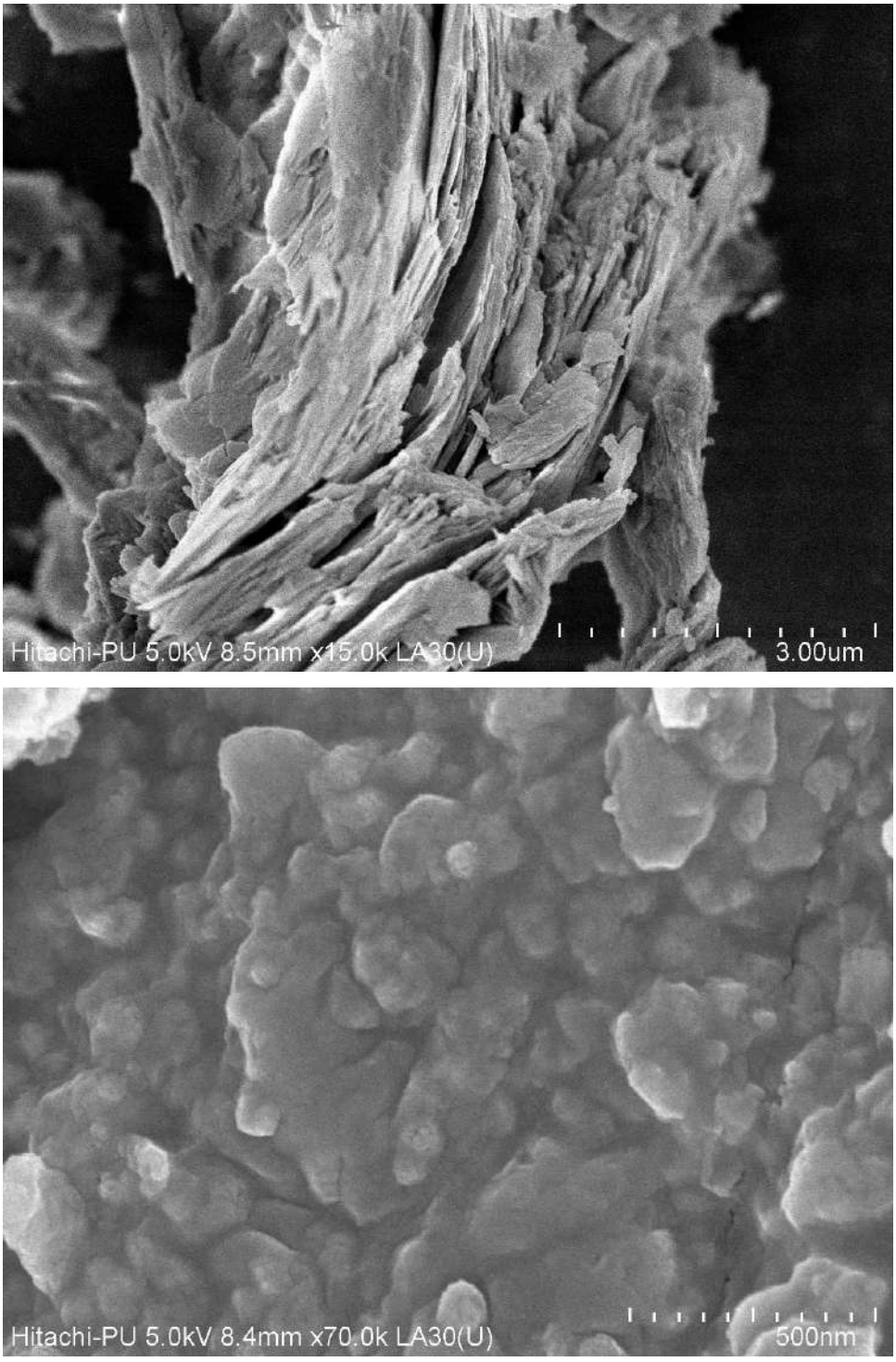

FIGURE 5c

Fig. 5: FE-Scanning electron microscopic micrographs of (a) $Zn_{0.9}Gd_{0.1}O$ (b) $Zn_{0.99}Gd_{0.01}O$ and (c) ZnO nanocrystals

3.5 OPTICAL STUDIES

Figure 6 presents the UV-Visible absorption spectra for pure and Gd-doped ZnO nanoparticles. A small shift to longer wavelength (red shift) was observed in the absorption edges upon doping with Gadolinium. Furthermore, the shift in wavelength is directly related to the size of nanoparticles as calculated from XRD data. The absorption edges are observed at 367 nm, 369 nm, 369 nm, 370 nm, 367 nm and 366 nm for $Zn_{0.9}Gd_{0.1}O$, $Zn_{0.99}Gd_{0.01}O$, $Zn_{0.999}Gd_{0.001}O$, $Zn_{0.9999}Gd_{0.0001}O$, $Zn_{0.99999}Gd_{0.00001}O$ and ZnO nanoparticles respectively. This data is used to determine the band gap energy (E_{bg}) of above mentioned nanoparticles using the equation (6).

$$E_{bg} = \frac{hc}{\lambda} \qquad (6)$$

Where h is Planck's constant, $c$is the velocity of light and λ is the absorption wavelength(nm). The value of the band gap obtained for $Zn_{1-x}Gd_xO$ ($0.000001 \leq x \leq 0.1$) nanoparticles are 3.38 eV, 3.36 eV, 3.36 eV, 3.35 eV, 3.38 eV and 3.39 eV for x = 0.10000, 0.01000, 0.00100, 0.00010, 0.00001 and 0.00000, respectively. As the doping gadolinium ions can produce new electronic levels inside the ZnO band gap, thus supports the decreased band gap energy value upon doping.

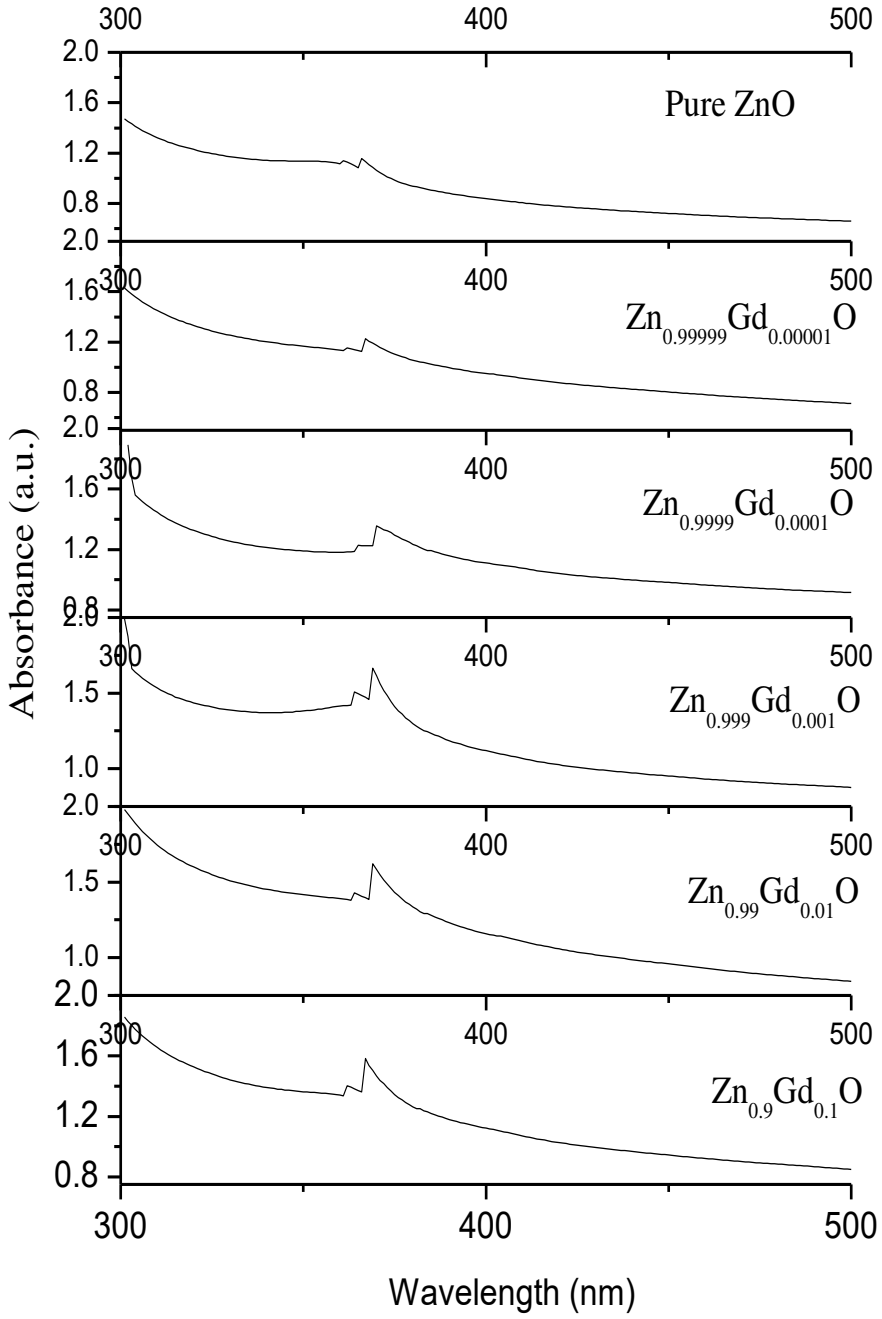

Fig. 6: Absorbance spectra of PVP capped ZnO and $Zn_{1-X}Gd_XO$ ($0.00001 \leq X \leq 0.1$) Nanoparticles

3.6 PHOTOCATALYTIC BEHAVIOR

MO dye is an aromatic compound with azo group and its molecular formula is $C_{14}H_{14}N_3NaO_3S$. The IUPAC name of methyl orange dye is Sodium4[(4dimethylamino)phenyldiazenyl]benzenesulfonate and colour code number is 13025. It is among the commonly used dyes in textile industry and is a highly toxic chemical. It may cause respiratory, eye and skin irritation. Various textile industries release large amount of MO dyes as colored wastewater in natural water resources that make water toxic and hazardous for aquatic flora and fauna. Degradation of MO dye into harmless compounds using ZnO nanophotocatalysts is a highly efficient and cost effective method [35-37]. The present experiments show the Photocatalytic efficiency of ZnO nanoparticles have enhanced by its doping with gadolinium. Photocatalytic degradation of methyl orange dye was examined using PVP capped $Zn_{1-x}Gd_xO$ nanostructures under UV irradiation using optical absorption spectroscopy. Although the IR studies have confirmed the presence of acetate groups in pure and Gd-doped ZnO nanoparticles which may reduce the photocatalytic efficiency[38], yet an efficient Photocatalytic degradation of MO dye is observed in the presence of prepared nanoparticles. Absorption spectra of methyl orange dye without nanocatalyst before and after UV radiation exposure is shown Fig. 7 for comparison.

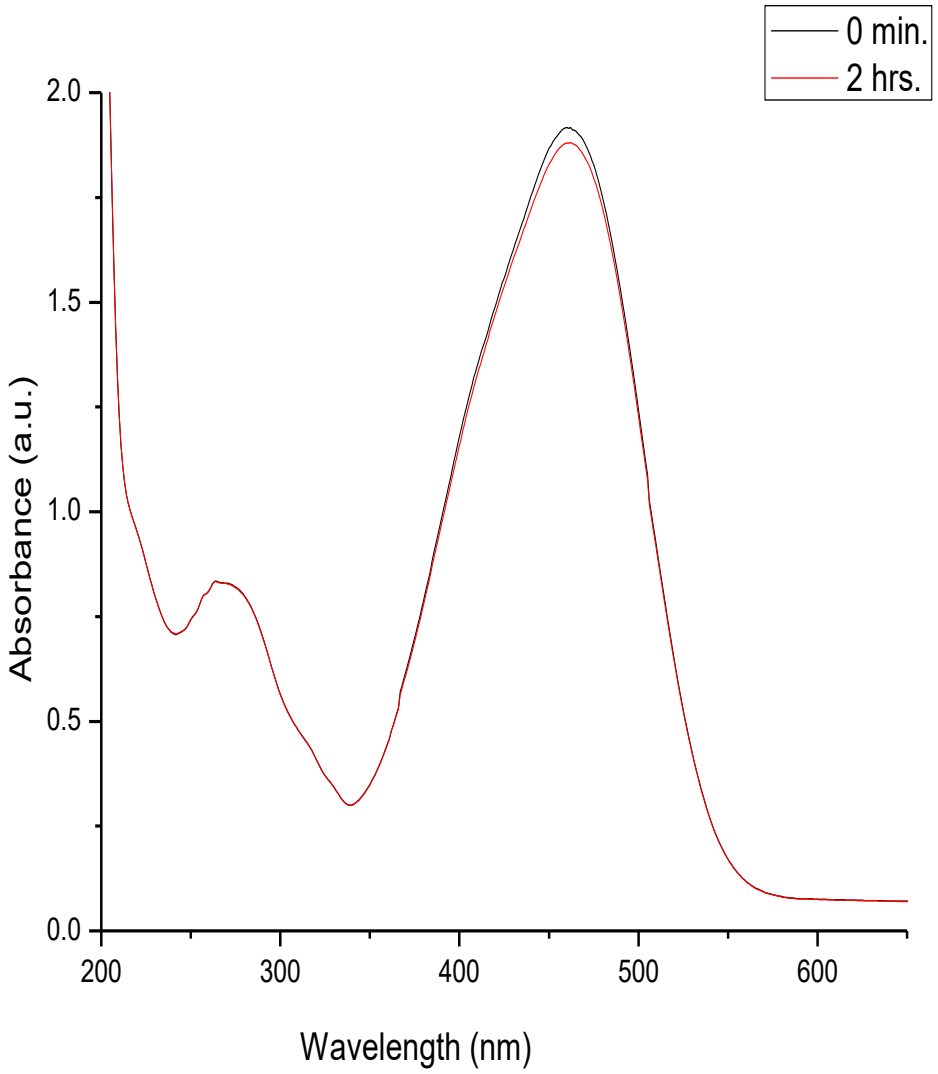

Fig. 7: Ultraviolet-Visible spectra of the methyl orange dye in aqueous solution upon irradiation with ultraviolet light.

Absorption peaks were absorbed at 264 nm and 462 nm in the spectrum. Out of these two, peak at 462 nm was used to study the dye degradation in the presence of UV light and nanocatalyst. Absorption spectra have shown a negligible change even after 2 h irradiation. It clearly indicates that aqueous methyl orange dye cannot be degraded by UV light alone in the absence of nanocatalyst. The absorption spectrum of dye degradation in the presence of $Zn_{0.999900}Gd_{0.000100}O$ nanocatalyst and UV light is presented in Figure 8.

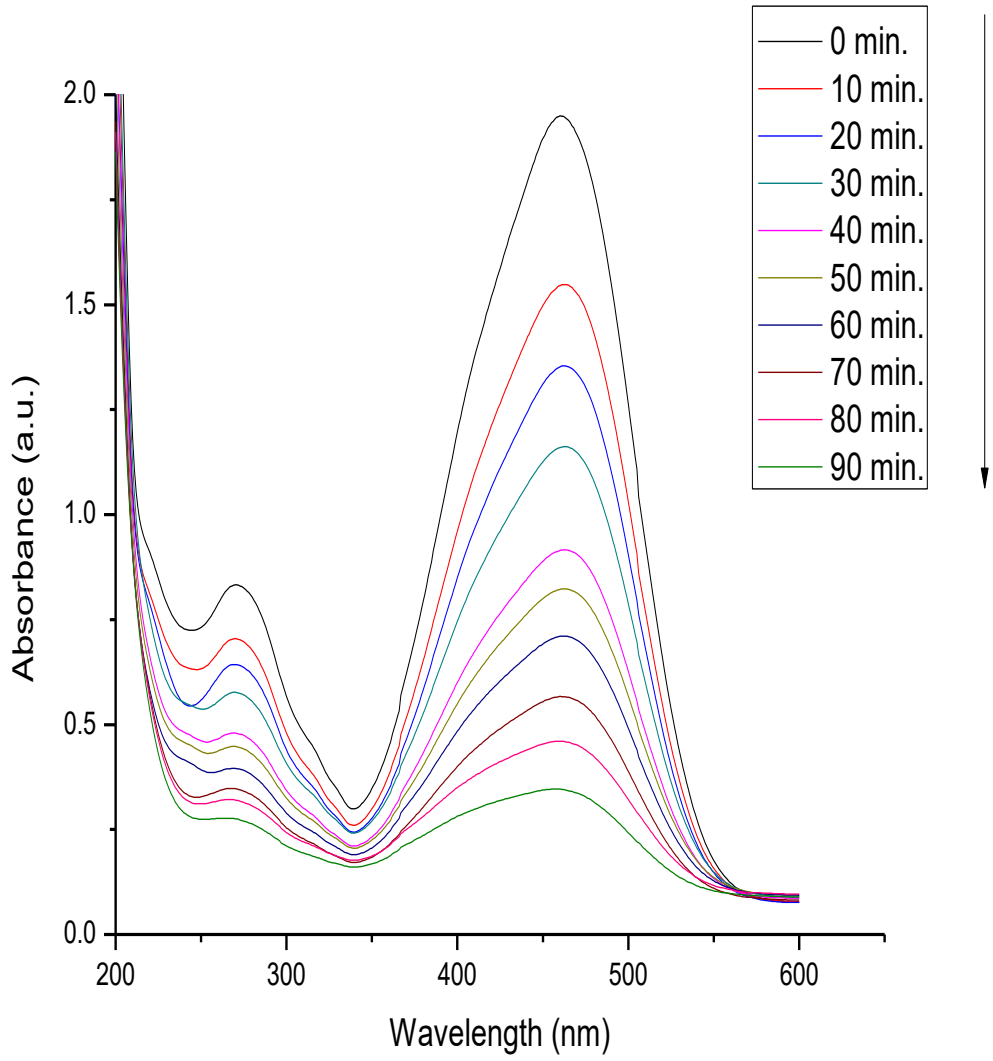

Fig. 8: Absorption spectra of MO dye under UV light irradiation in the presence of $Zn_{0.9999}Gd_{0.0001}O$ nanocrystals

These results clearly show that aqueous methyl orange solution was degraded by the addition of $Zn_{1-x}Gd_xO$ nanophotocatalyst. Figure 9a and 9b represents the plots of dye concentration versus the UV irradiation time (t) and

plots of $\ln(C_0/C_t)$ versus the UV irradiation time (t) respectively for pure and Gd-doped ZnO nanopowders. Plots of $\ln(C_0/C_t)$ versus the UV irradiation time (t) suggest that the photodegradation of methyl orange dye follows the pseudo-first order kinetics.

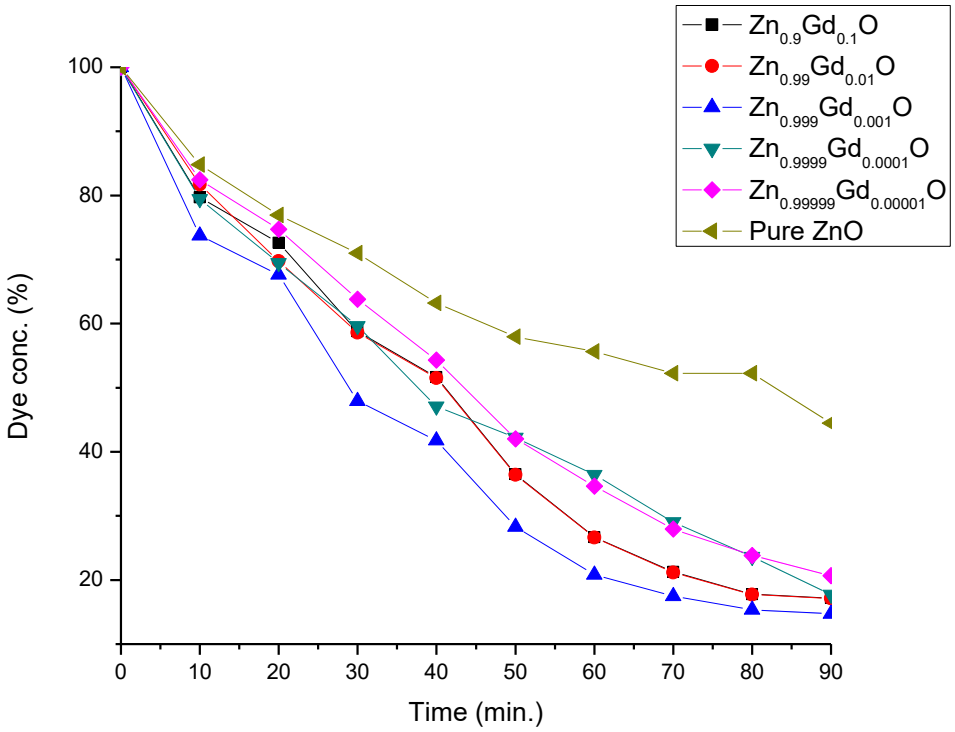

Fig. 9a Plots of dye concentration versus the UV irradiation time (T)

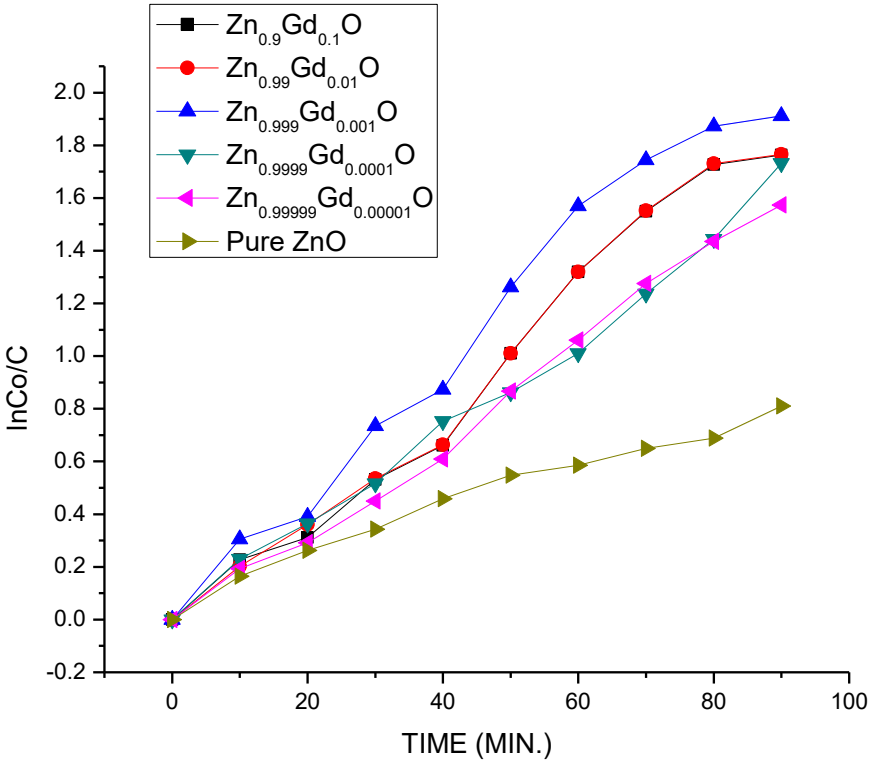

Fig 9b: Plots of ln(C_0/C_t) versus the UV irradiation time (T)

The values of first-order rate constants (k) are 1.96×10^{-2} min^{-1}, 1.96×10^{-2} min^{-1}, 2.12×10^{-2} min^{-1}, 1.92×10^{-2} min^{-1}, 1.75×10^{-2} min^{-1} and 0.9×10^{-2} min^{-1} where as the degradation efficiency (ε) values are 82.83%, 82.89%, 85.30%, 82.30%, 79.33% and 55.50% for various $Zn_{1-x}Gd_xO$ nanoparticles with x = 0.10000, 0.01000, 0.00100, 0.00010, 0.00001 and 0.00000, respectively as listed in table 4. The photocatalytic performance is directly proportional to the value of apparent rate constants (k) calculated from the linear fitted curves using Eq. (4). After comparing the values of k, it can be stated that the doping of ZnO with gadolinium has significantly increased its photocatalytic efficiency. Among various doped Zn O nanomaterials, the increasing order The maximum increase is noted in case of $Zn_{0.99900}Gd_{0.00100}O$ nanocrystals (ε= 85.3% and k = 2.12 × 10^{-2} min^{-1}) whereas it is minimum in case of $Zn0._{99999}Gd_{0.00001}O$ nanocrystals (ε = 79.3% and k = 1.75 × 10^{-2} min^{-1}).

Samples $Zn_{1-x}Gd_xO$	Rate constant (k) in min^{-1}	Degradation efficiency (Є) in %
$x = 0.10000$	1.96×10^{-2}	82.83
$x = 0.01000$	1.96×10^{-2}	82.89
$x = 0.00100$	2.12×10^{-2}	85.30
$x = 0.00010$	1.92×10^{-2}	82.30
$x = 0.00001$	1.75×10^{-2}	79.33
$x = 0.00000$	0.9×10^{-2}	55.50

Table 4: Photocatalytic decolorization rate constants and degradation efficiency of methyl orange dye using pure and Gd-doped ZnO nanophotocatalysts under UV irradiation

Photocatalytic degradation scheme of MO dye under UV light irradiation in the presence of Gd-doped ZnO nanoparticles occurs by following proposed mechanism:

STEP I: Absorption of light by Gd doped ZnO nanoparticles that excite electron from valence band to conduction band thus creating a positive hole in valence band.

STEP II: Positive holes react with hydroxyl ions produced by ionization of chemisorbed water molecules to produce $OH^{\cdot}$ radicals, whereas electrons in conduction band reduce oxygen to form superoxide radical $O_2^{\cdot}$.

STEP III: $OH^{\cdot}$ radicals, being strong oxidizing agents, react with organic dye and cause its complete mineralization as indicated by decolorization of its intense orange colored aqueous solution.The complex dye molecule undergoes demethylation, oxidation and hydroxylation process results in the formation of simplemolecules and ions namelycarbon dioxide, water, sulphate ions and nitrate ions.

The photocatalytic activity of photocatalysts largely depends upon the reducing tendency of electron hole recombination. Presence of various intrinsic and extrinsic defects in such compounds has significantly increased the separation time for electron hole recombination. Intrinsic defects namely oxygen vacancies are the characteristic features of ZnO nanoparticles. Talking about extrinsic defects, doping of ZnO with Gd allows entry of Gd^{3+} into the crystal lattice of ZnO thus creating Zn^{2+} vacancy defects. These extrinsic and intrinsic defects in Gd doped ZnO nanostructures together retard the electron hole recombination time and inturn the photocatalytic efficiency of nanoparticles towards the degradation of methyl orange dye has increased.

CHAPTER – 4
CONCLUSIONS

Bottom up Chemical co-precipitation technique has been successfully employed for the synthesis of pure and Gd-doped ZnO nanoparticles using Polyvinyl Pyrrolidone as a capping agent. This method employed for synthesis is cost effective, time saving and a hassle free method. The insertion of Gd into ZnO has been confirmed from EDXRF studies, while the nanosize wurtzite structure has been revealed from XRD studies. Optical studies have revealed a decrease in band gap energy of zinc oxide nanoparticles upon doping with gadolinium.

Photocatalytic degradation of methyl orange dye in aqueous solution has studied under UV irradiation in the presence of prepared nanoparticles as catalyst. Methyl orange is an azo dye which is widely used in textile industry worldwide and is a major water pollutant. An efficient photocatalytic degradation of methyl orange dye into harmless products has been successfully achieved using synthesized nanoparticles as nano photocatalyst. It has been concluded that the catalytic efficiency of ZnO photocatalyst has enhanced upon doping with Gadolinium. Maximum degradation has achieved upon 0.1% doping of ZnO with Gd. 85% of the dye has been degraded in a very short span of time of 90 minutes using above said nano photocatalyst. Thus, the photocatalytic method of degradation of dyes in polluted water is quite efficient method.

BIBLIOGRAPHY

1. Rauf, M.A., Shehadeh, I., Ahmed, A., Al-Zamly, A., *Internat. J. Chem., Mol., Nuc., Mater. Metallurg. Eng* **2009**, *3(7)*, 369-374.
2. Catanho, M., Malpass, G.R.P., Motheo A.J., *Quimica Nova* **2006**, *29*, 983-989.
3. Faisal, M., Tariq, M.A., Muneer, M. *Dyes Pigm* **2007**, *72*, 233–239.
4. Kant, R. *J. Nat Sci.* **2012**, *4*, 22-26.
5. Zhang, T., Oyama, T., Horikoshi, S., Hidaka, H., Zhao, J., Serpone, N. *Solar Ener. Mater. Solar Cells* **2002**, *73(3)*, 287-303.
6. Sobczyński, A., and Dobosz, A. *Polish J. Environ. Studies*, **2001**, *10(4)*, 195–205.
7. Elmorsi, T.M., Riyad, Y.M., Mohamed, Z.H., Abid, H.M.H, Bary, E., *Journal of Hazardous Materials*, **2010**, *174*, 352-356.
8. Gul, S., Ozcan Yildlrln, O. *Chemical Engineering Journal*, **2009**, *155*, 684-690.
9. AlHamedi, F.H., Rauf, M.A., Asraf, S.S *Desalination*, **2009**, *239*, 159-166.
10. Wahab, R., Tripathy, S.K., Shin, H.S., Mohapatra, M., Musarrat, J., Khedhairy, A.A.A., Kaushik, N. K. *Chem. Eng. J.*, **2013**, *226*, 154–160.
11. Kansal, S.K., Ali, A.H., Kapoor, S. *Desalination*, **2010**, *259(1-3)*, 147–155.
12. Kajbafvala, A., Ghorbani, H., Paravar, A., Samberg, J.P., Kajbafvala, E., Sadrnezhaad, S.K. *Superlattice Microst.*, **2012**, *51(4)*, 512–522.
13. Chen, P.K., Lee, G.J., Davies, S.H., Masten, S.J., Amutha, R., Wu, J.J. *Mater. Res. Bull.*, **2013**, *48(6)*, 2375–2382.
14. Xu L., Li Z., Cai Q., Wang H., Gao H., Lv, W. Liu, J. *Cryst Eng Comm*, **2010**, *12*, 2166–2172.
15. Senthilraja, A., Subash, B., Krishnakumar, B., Rajamanickam, D., Swaminathan, M., Shanthi, M. *Mater. Sci. Semicond. Process.*, **2014**, *22*, 83–91.
16. Wu, H., Pan, W. *J. Am.Ceram. Soc*, **2006**, *89*, 699–701
17. Gouvea, C.A.K., Wypych, F., Moraes, S.G., Duran, N., Peralta-Zamor, P. *Chemosphere*, **2000**, *40(4)*, 427–432.
18. Elamin, N., Elsanousi A., *J. App. and Industrial Sci.*, **2013**, *1*, 32-35.

19. Xiao, Q., Ouyang, L. *J. Alloy. Compd.*, **2009**, *479 (1-2)*, 4-7.
20. Zhi-gang, J., Kuan-kuan, P., Yan-hua, L.I., Rongsun, Z. *Trans. Nonferrous Met. Soc. China.*, **2012**, *12*, 873−878.
21. Ekambaram, S., Iikubo, Y., Kudo, A. *J. Alloy. Compd.*, **2007**, *433 (1-2)*, 237–240.
22. Min, F., Li, Y., Siwei, W., Peng, L., Liu, J., Dong, F., *Appl. Surf. Sci.*, **2011**, *258(4)*, 1587–1591.
23. Abbad, M.M.B., Kadhum, A.A.H., Mohamad, A.B., Takriff, M.S., Sopian, K. *Chemosphere*, **2013**, *91(11)*, 1604–1611.
24. Vaiano V., Matarangolo M., Sacco O., Sannino D. *Chemical Engineering Transactions*, **2017**, *57*, 625-630.
25. Alam, U., Khan, A., Ali, D., Bahnemann, D., Muneer, M. *RSC Adv.*, **2018**, *8*, 17582–17594.
26. Jun-Lian, C., Neena, D., Na, L., De-Jun, F., Xian-Wen, K. *Chinese Physics B*, **2018**, *27(8)*, 086102.
27. Hu, B., Sun, Q., Zuo, C., Pei, Y., Yang, S., Zheng, H., Liu, F. *Beilstein J. Nanotechnol.*, **2019,** *10,* 1157–1165.
28. Parangusan, H., Ponnamma,D.,Al-maadeed. M. A. A. *Bull. Mater. Sci.* **2019**, *42*, 179.
29. Samanta, A., Goswami, M.N., Mahapatra, P, K. *Materials Research Express*, **2019**, *6*, 065031.
30. Pascariu, P., Cojocaru, C., Olaru, N., Samoila, P., Airinei, A., Ignat, M., Sacarescu, L., Timpu, D. *J. Environmental Management*, **2019**, *239*, 225-234.
31. Laidler,K.J., Meiser, J.H., *Physical Chemistry*, **1982**, *ISBN 0-8053-5682-7*, 780.
32. Joint Committee on Powder Diffraction Standards (JCPDS) File No. 05-0664.
33. Rajendar, V., Dayakar, T., Shobhan, K., Srikanth, I., Rao, K.V. *Superlatt. Microstruc.*, **2014**, *75*, 551–563.
34. Rao, C.N.R. Chemical Applications of Infrared spectroscopy, Academic Press, New York and London, **1963**.
35. Chowdhury, M. I. H., Hossain, M. S., Azad, M. A. S., Islam, M. Z., Dewan, M.A. *IJSER*, **2018**, *9(6)*, 1646-1649.
36. Chen, X., Wu, Z., Liu, D., Gao, Z. *Nanoscale Res Lett*, **2017,** *12***,** 143.

37. Ghule, L. A., Patil, A. A., Sapnar, K. B., Dhole, S. D., Garadkar, K. M. *Toxicological & Environmental Chemistry*, **2011**, *93(4)*, 623-634.

38. Giraldi, T. R., Santos, G. V. F., Mendonça, V. R., Ribeiro, C., Weber, I. T. *J. Nanosci. Nanotechnol.*, **2011**, *11(4)*, 43635–3640.

Chemical Physics Letters 746 (2020) 137302

Contents lists available at ScienceDirect

Chemical Physics Letters

journal homepage: www.elsevier.com/locate/cplett

Research paper

Photocatalytic degradation of methyl orange dye under UV irradiation in the presence of synthesized PVP capped pure and gadolinium doped ZnO nanoparticles

Rupy Dhir

Department of Chemistry G.S.S.D.G.S. Khalsa College, Patiala, Punjab, India

HIGHLIGHTS

- Synthesis of $Zn_{1-x}Gd_xO$ nanoparticles using wet chemical co-precipitation technique.
- Polyvinylpyrrolidne was used as a capping agent.
- The synthesized nanoparticles were used as photocatalysts for the degradation of methyl orange dye.
- Doping of ZnO nanoparticles has greatly increased its catalytic efficiency.

ARTICLE INFO

Keywords:
Nanophotocatalysts
Chemical co-precipitation
Doping

ABSTRACT

The present study focuses on the development of efficient nanophotocatalysts (pure and Gadolinium doped Zinc oxide) for the degradation of methyl orange dye in polluted water. Chemical co-precipitation technique was employed for the synthesis of target compounds using zinc acetate and gadolinium nitrate as metal precursors. The synthesized nanoparticles were characterized by various spectroscopic techniques namely X-ray diffraction, Fourier Transform infra red spectroscopy, Field emission scanning electron microscopy and energy dispersive X-ray spectroscopy. The synthesized pure and Gadolinium doped Zinc oxide nanoparticles were used as photocatalysts for the degradation of methyl orange dye under ultra-violet light irradiation. Doping of ZnO nanoparticles with Gadolinium has greatly increased its catalytic efficiency.

1. Introduction

Water pollution is one of the major environmental challenges, humankind is facing these days. The dyes which are widely used in textile, plastic, medicine and many other industries are the main cause of water pollution [1]. Azo dyes such as methyl orange constitutes about half of textile dyes [2]. The presence of these dyes in water sources contribute to toxicity, eutrophication and hinder the infiltration of sunlight, thus severely affect the growth of aquatic life [3] and causing long-term health effects [4]. Current methods including conventional sewage plant treatment [5] do not degrade harmful chemicals present in dyes and only insufficiently remove them from polluted water. An alternative and highly efficient technique for the degradation of dye is photocatalysis using semiconductor photocatalysts [6–9]. The photocatalysts are the substances that chemically react with dyes in the presence of light and convert them into non toxic products by oxidation process. Comparing the photocatalytic activity of various semiconductor photocatalysts in aqueous media, zinc oxide (ZnO) is found to be on top position [10,11] and its photocatalytic activity can be further enhanced by moving from bulk to nano ZnO. [12]. It is because of large surface area of nanomaterials thus produces large number of active sites. Doping of ZnO nanomaterials further increases its photocatalytic efficiency towards the degradation of dyes [13–23]. Literature study has revealed that doping of ZnO nanoparticles with rare earth metal atoms have significantly increased its photocatalytic efficiency towards the degradation of organic dyes in water [24–30]. Doping introduces another metal ions by substituting Zn ions from their original lattice points and produces traps photogenerated charge carriers which inturn lower the electron hole pair recombination rate, hence increases the photocatalytic efficiency.

To best of my knowledge, studies on the photocatalytic degradation of methyl orange dye using Gadolinium doped (Gd-doped) ZnO nanoparticles are scarce in literature. So, in the present investigation, Gd-doped ZnO nanoparticles were synthesized by chemical co-precipitation method using zinc acetate and gadolinium nitrate as metal precursors. The synthesized nanoparticles were characterized by various

E-mail address: rupydhir431@yahoo.com.

https://doi.org/10.1016/j.cplett.2020.137302
Received 15 December 2019; Received in revised form 1 February 2020; Accepted 2 March 2020
Available online 08 March 2020
0009-2614/

spectroscopic techniques namely X-ray diffraction (XRD), Fourier Transform infra red spectroscopy (FT-IR), Field emission scanning electron microscopy (FESEM), energy dispersive X-ray spectroscopy (EDXRF) and optical studies. (PC) degradation of methyl orange dye was studied in aqueous medium in the presence of synthesized nanoparticles under the irradiation of UV light.

2. Experimental procedure

2.1. Materials

Gadolinium (III) nitrate hexahydrate (99.9%) was purchased from Sigma Aldrich. Co, 3050, St. Louis, MO, USA, Zinc acetate, sodium hydroxide, polyvinyl pyrrolidone and methyl orange were of analytical reagent grade and used without further purification. All solutions used in the experiments were prepared by using triply distilled deionised water.

2.2. Synthesis of $Zn_{1-x}Gd_xO$ nanoparticles

Pure and gadolinium doped ZnO nanoparticles ($Zn_{1-x}Gd_xO$, $0.00001 \leq x \leq 0.1$) were prepared using bottom up wet chemical co-precipitation technique in the presence of polyvinyl pyrrolidone (PVP) as a capping agent. Synthesis was carried out under ambient conditions. In the typical synthetic procedure, stoichiometric proportion of 0.5 M zinc acetate was taken in a titration flask followed by drop wise addition of gadolinium nitrate solution. After stirring the mixture for 1 h, 8 ml. of 2% PVP was added and then 0.5 M sodium hydroxide solution was added drop wise with continuous stirring. Resulting white precipitates were filtered, thoroughly washed and then dried in hot air oven at 150 °C temperature for one hour followed by crushing using mortar and pestle to obtain nanoparticles in fine powder form. The amount of precursors solution used for preparation of Gd-doped ZnO samples is listed in Table 1. Eq. (1) and (2) represents the stepwise formation of ZnO nanoparticles.

$$Zn(CH_3COO)_2(aq.) + 2NaOH(aq.) + \overset{PVP}{\rightarrow} Zn(OH)_2(s) + 2CH_3COONa(aq.) \quad (1)$$

$$Zn(OH)_2(s) \overset{Heat}{\rightarrow} ZnO + H_2O \quad (2)$$

2.3. Characterization

The synthesized Gd-doped ZnO nanoparticles have been characterized using X-ray diffraction, FE scanning electron microscopy, Fourier Transform infrared spectroscopy and energy dispersive x-ray fluorescence techniques. X-ray diffraction spectrum is obtained from powder X-ray diffraction (PAN-Analytic) setup using 3050/60 goniometer and Cu anode X-ray tube. The X- ray diffraction scans were performed in the 2θ range 20–80° keeping step size 0.001for the Cu K X-ray radiation (λ = 1.5406 Å) at 40 mA–45 kV generator setting for the powder samples. For average particle size determination FE scanning electron microscopic micrographs at an accelerating voltage of 5 kV with magnification of 70,000 were taken using Hitachi (SU8000) FE scanning electron microscope. The energy dispersive x-ray fluorescence technique is used for elemental and compositional analysis of synthesized nanomaterials. Energy dispersive x-ray fluorescence spectrometer involving Mo anode X-ray tube (PAN-Analytic) as an excitation source and LEGe (Canberra made, FWHM = 150 eV at 5.89 keV) as photon detector is used to record spectra of the Gd doped ZnO nanomaterials. Fourier Transform Infrared studies were performed using Bruker alfa Fourier Transform Infrared spectrometer.

Table 1
Amount of precursors used in sample preparation.

Sample details $Zn_{1-x}Gd_xO$	Amounts of precursors used in sample preparation		
	Volume of 0.5 M Zn $(OCOCH_3)_2$ solution (ml)	Volume of 0.5 M NaOH solution (ml)	Volume of Gd $(NO_3)_3{\cdot}6H_2O$ (M) solution (ml)
$x = 0.1$	45	50	1.04 (1 M)
$x = 0.01$	49.5	25	1.04 (0.1 M)
$x = 0.001$	49.95	25	1.04 (0.01 M)
$x = 0.0001$	49.995	25	1.04 (0.001 M)
$x = 0.00001$	49.9995	25	1.04 (0.0001 M)
$x = 0.0$	50	25	–

2.4. Photocatalytic behaviour

The photocatalytic behaviour of pure ZnO and Gd-doped ZnO nanomaterials were studied under UV light exposure for the degradation of methyl orange dye in aqueous medium using UV-photoreactor [dimension of 1 ft (height) × 0.5 ft (length)] equipped with one 160 W UV-bulb (OSRAM made 468). The distance between the reactor setup and UV-tube was ~10 cm. 100 mg nanopowder mixed with 250 ml of 16 ppm methyl orange dye solution in a glass reactor with surface area 50 cm^2 was used for photocatalytic studies. For first one hour the above solution was put under constant stirring in dark for the adsorption of dye molecules on the surface of nanoparticles. It was then exposed to the ultraviolet-radiation with continuous magnetic stirring. 10 ml of suspension solution was sampled and centrifuged at fixed time intervals. After centrifugation, the supernatant was analyzed using the ultraviolet–visible spectrophotometer. The concentration of dye was measured from the optical absorption values at a certain wavelength. The equation (3) represents the degradation efficiency (ε) of dye

$$\in = \frac{Co - C}{Co} \times 100 \quad (3)$$

where as C_o and C represent the initial concentration of the dye the concentration after UV irradiation respectively. Furthermore, in accordance to the Langmuir–Hinshelwood kinetics model [31], the photocatalytic process of methyl orange dye can be expressed as apparent pseudo-first-order kinetic Eq. (4).

$$ln\frac{Co}{C} = \kappa t \quad (4)$$

where κ is the apparent pseudo-first-order rate constant, C_o is original methylene blue concentration and C is methylene blue concentration in aqueous solution at time t.

3. Results and discussion

3.1. Crystallographic characterization

Fig. 1a represents the XRD patterns of all the synthesized pure and gadolinium doped ZnO nanoparticles ($Zn_{1-x}Gd_xO$, $0.00001 \leq x \leq 0.1$). The successful synthesis, crystalline nature and hexagonal wurtzite structure of ZnO nanoparticles is confirmed from various sharp peaks in XRD graph observed at 2θ of 31.76°, 34.39, 36.22, 47.52, 56.54, 62.81, and 67.84 correspond to lattice planes (1 0 0), (0 0 2), (1 0 1), (1 0 2), (1 1 0), (1 0 3) and (1 1 2) respectively as reported in JCPDS file no. 05-0664 [32]. The lattice parameters 'a' and 'c' identified by JCPDS for hexagonal wurtzite ZnO are 3.2498 Å and 5.2066 Å respectively. Any diffraction peak related to impurity phase is not detected which indicates the successful substitution of Gd^{3+} ions into Zn^{2+} sites without disturbing wurtzite crystal structure of ZnO. The shifting of peaks shown in Fig. 1b indicates the substitution of Gd in the crystalline ZnO structure. This is due to the expansion of ZnO lattice upon doping with Gadolinium as the ionic radii of Gd^{3+} (0.94 Å) is larger than that of Zn^{2+} (0.74 Å).

Scherrer'r formula [33] Eq. (5), by estimating full width at half

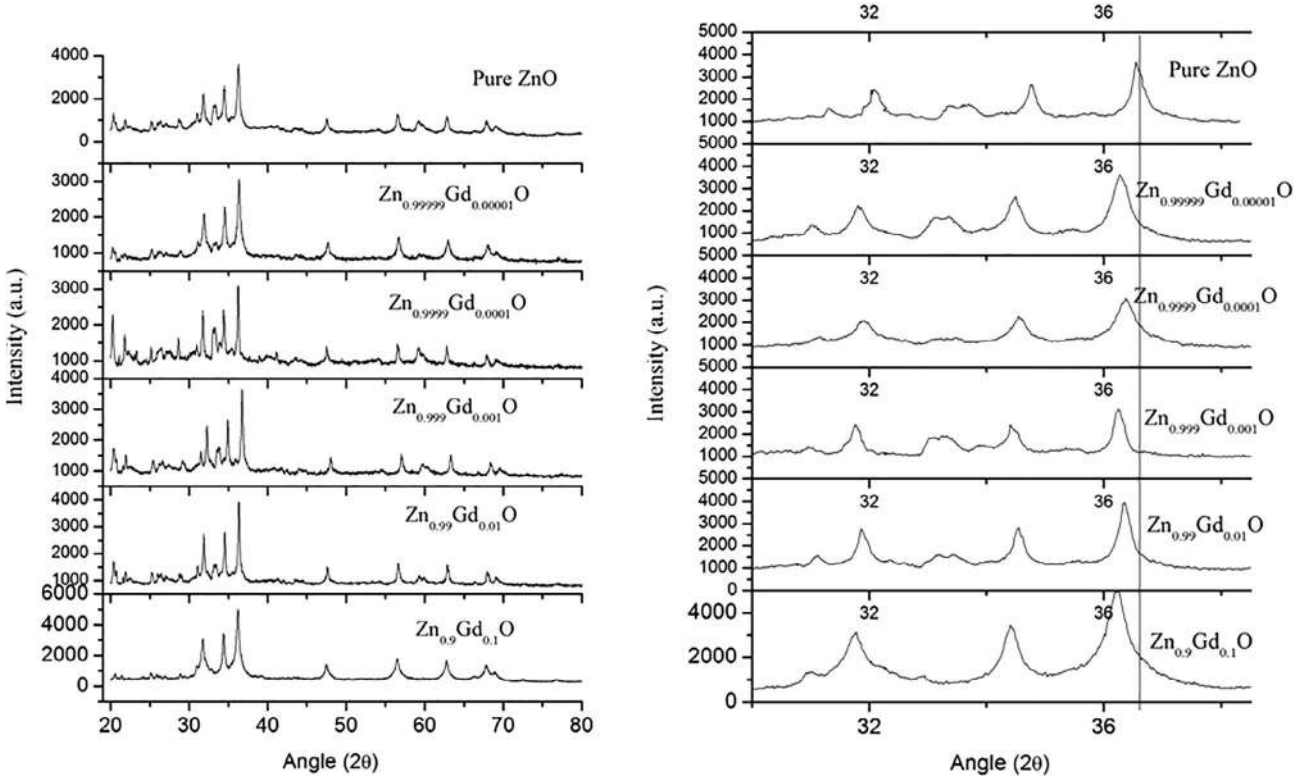

Fig. 1. X- ray diffraction spectra of PVP capped ZnO and $Zn_{1-x}Gd_xO$ ($0.00001 \leq x \leq 0.1$) nanoparticles (a) Angle (2θ) ranges from 20 to 80 (b) Angle (2θ) ranges from 30 to 38.

maximum (FWHM) of sharp peak (1 0 1), was used to calculate the average crystalline size of the prepared nanoparticles.

$$D = \frac{0.89\lambda}{\beta\cos\theta} \quad (5)$$

where λ represents the wavelength of Cu K α radiation, β represents the diffraction peak's full width half maxima, and θ is the Bragg peak angle. The estimated crystalline sizes of $Zn_{1-x}Gd_xO$ ($0.000001 \leq x \leq 0.1$) nanoparticles at most intense crystallographic plane [1 1 0] are found 11.49 nm, 37.94 nm, 41.05 nm, 52.67 nm, 20.38 nm and 18.62 nm for × = 0.10000, 0.01000, 0.00100, 0.00010, 0.00001 and 0.00000 respectively.

3.2. Fourier Transform infrared (FTIR) spectroscopic studies

Fig. 2 represents FTIR spectra of pure and Gd-doped ZnO nanoparticles. The peaks observed at 3471 and 1396 cm^{-1} are assigned to O-H stretching and deformation respectively and is attributed to water adsorption on the metal surface. Due to inter-atomic vibrations, metal oxides generally exhibit absorption bands in fingerprint region i.e. below 1000 cm^{-1}. The peak at 668 is corresponded to Zn-O stretching vibration, which is in accordance with literature values [34]. Various absorption peaks between 900 and 2900 cm^{-1} are also recorded in all samples. Absorption peaks around 900–1020 cm^{-1}, 1300–1600 cm^{-1} and 2850–2950 cm^{-1} are assigned to C–C stretching mode, C–O stretching modes (symmetric and asymmetric) and C–H bond of the acetate group respectively. The above observation and discussion indicates the presence of hydroxy and acetate groups on the surface of pure and Gd-doped ZnO nanoparticles.

3.3. Energy dispersive X-ray fluorescence (EDXRF) studies

Fig. 3a-3d represent the chemical compositions of the prepared pure and gadolinium doped ZnO nanoparticles ($Zn_{1-x}Gd_xO$,

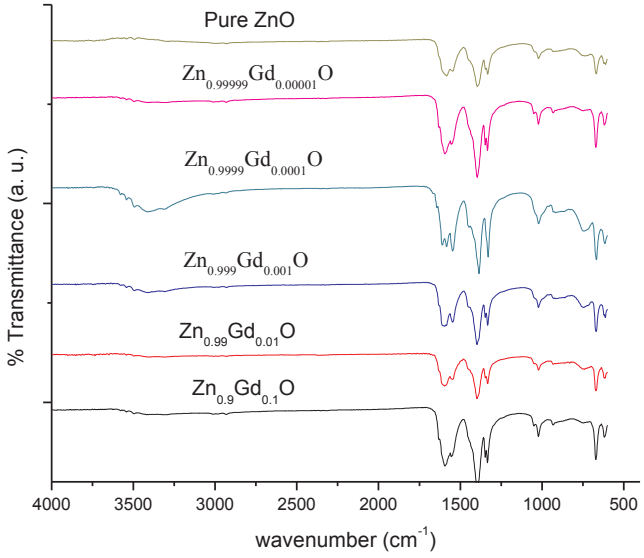

Fig. 2. Fourier Transform Infrared spectra of polyvinyl pyrrolidone capped $Zn_{1-x}Gd_xO$ (x = 0, 0.000001, 0.00001, 0.0001, 0.001, 0.01 and 0.1) nanocrystals.

$0.001 \leq x \leq 0.1$) measured by EDS spectra. From the spectra 3a-3c, the presence of Zn, O and Gd is confirmed in Gd doped ZnO NPs whereas the spectrum 3d of pure ZnO NPs confirmed the presence of only zinc and oxygen ions. The obtained EDS result confirms the doping of ZnO matrix with Gd. The percentage amount of Gd calculated from EDS studies in $Zn_{1-x}Gd_xO$ samples is 1.02, 0.18 and 0.05 against theoretical value of 1, 0.1 and 0.01 for × = 0.01, 0.001 and 0.0001 respectively. The experimental values are in good agreement with the calculated values.

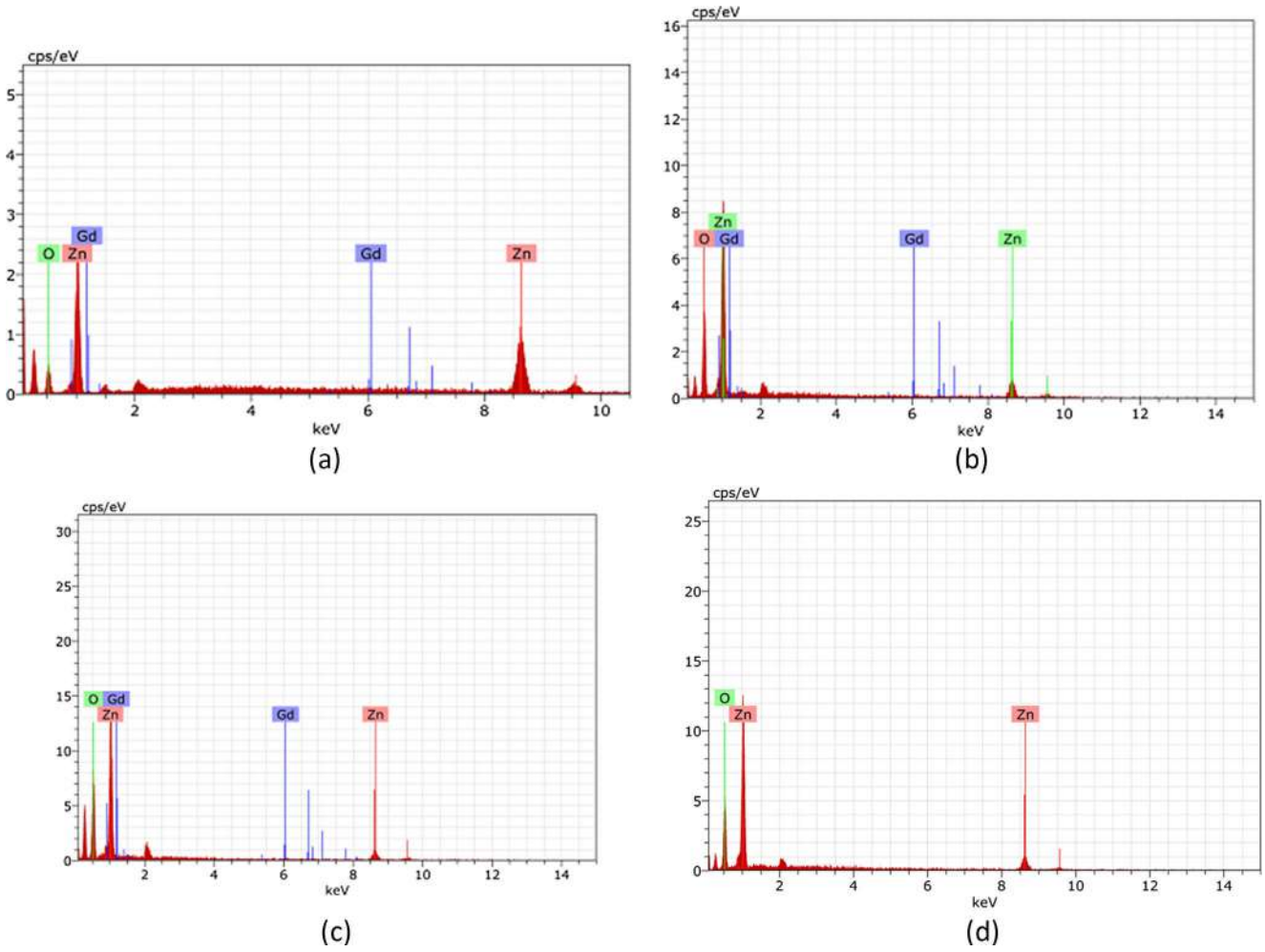

Fig. 3. Energy dispersive x-ray fluorescence spectra of $Zn_{1-x}Gd_xO$ nanocrystals. (a) x = 0.01, (b) x = 0.001, (c) x = 0.0001, (d) x = 0.

3.4. FE scanning electron microscopic studies

The surface morphology of the PVP capped pure and Gd-doped ZnO nanoparticles were examined with FE scanning electron microscope. FE-SEM micrographs of pure ZnO Fig. 4a and $Zn_{0.9}Gd_{0.1}O$ Fig. 4b nanoparticles show spherical clusters of particles. However, the doping with gadolinium results in a decrease in size of clusters.

3.5. Optical studies

Fig. 5 presents the UV–Visible absorption spectra for pure and Gd-doped ZnO nanoparticles. A small shift to longer wavelength (red shift) was observed in the absorption edges upon doping with Gadolinium. Furthermore, the shift in wavelength is directly related to the size of nanoparticles as calculated from XRD data. The absorption edges of $Zn_{1-x}Gd_xO$ ($0.000001 \leq x \leq 0.1$) nanoparticles are 367 nm, 369 nm, 369 nm, 370 nm, 367 nm and 366 nm for × = 0.10000, 0.01000,

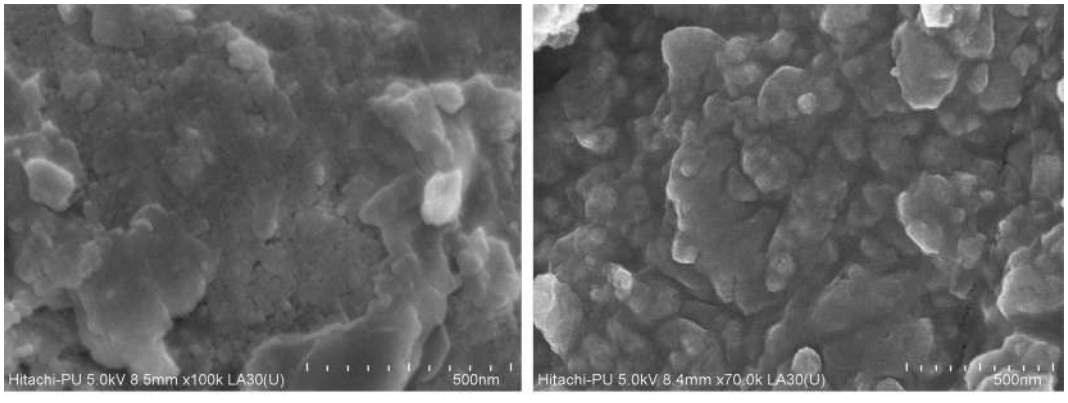

Fig. 4. FE-Scanning electron microscopic micrographs of (a) $Zn_{0.9}Gd_{0.1}O$ and (b) ZnO nanocrystals.

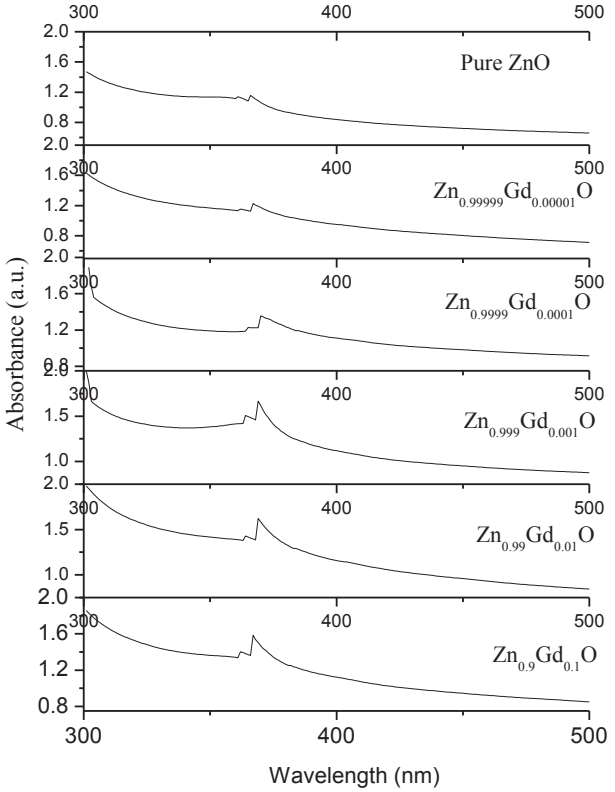

Fig. 5. Absorbance spectra of PVP capped ZnO and $Zn_{1-x}Gd_xO$ ($0.00001 \leq x \leq 0.1$) nanoparticles.

0.00100, 0.00010, 0.00001 and 0.00000, respectively. This data is used to determine the band gap energy of pure and Gd-doped ZnO nanoparticles using the equation (6).

$$E_{bg} = \frac{hc}{\lambda} \tag{6}$$

where E_{bg} is the band gap energy, h is Planck's constant (4.135667×10^{-15} eV s), c is the velocity of light (2.997924×10^{8} m/s), and λ is the absorption wavelength (nm). The value of the band gap obtained for $Zn_{1-x}Gd_xO$ ($0.000001 \leq x \leq 0.1$) nanoparticles are 3.38 eV, 3.36 eV, 3.36 eV, 3.35 eV, 3.38 eV and 3.39 eV for × = 0.10000, 0.01000, 0.00100, 0.00010, 0.00001 and 0.00000, respectively. As the doping gadolinium ions can produce new electronic levels inside the ZnO band gap, thus supports the decreased band gap energy value upon doping.

3.6. Photocatalytic behavior

MO dye is an aromatic compound with azo group and its molecular formula is $C_{14}H_{14}N_3NaO_3S$. The IUPAC name of methyl orange dye is Sodium4[(4dimethylamino)phenyldiazenyl]benzenesulfonate and colour code number is 13025. It is among the commonly used dyes in textile industry and is a highly toxic chemical. It may cause respiratory, eye and skin irritation. Various textile industries release large amount of MO dyes as colored wastewater in natural water resources that make water toxic and hazardous for aquatic flora and fauna. Degradation of MO dye into harmless compounds using ZnO nanophotocatalysts is a highly efficient and cost effective method [35–37]. The present experiments show the Photocatalytic efficiency of ZnO nanoparticles have enhanced by its doping with gadolinium.

Photocatalytic degradation of methyl orange dye was examined using PVP capped $Zn_{1-x}Gd_xO$ nanostructures under UV irradiation using optical absorption spectroscopy. Although the IR studies have confirmed the presence of acetate groups in pure and Gd-doped ZnO nanoparticles which may reduce the photocatalytic efficiency [38], yet an efficient Photocatalytic degradation of MO dye is observed in the presence of prepared nanoparticles. Absorption spectra of methyl orange dye without nanocatalyst before and after UV radiation exposure is shown Fig. 6a for comparison. Absorption peaks were absorbed at 264 nm and 462 nm, where as absorption peak at 462 nm was used to track the photocatalytic degradation process. Absorption spectra have shown a negligible change even after 2 h irradiation. It clearly indicates that aqueous methyl orange dye solution cannot be easily degraded by UV light. The absorption spectra of methyl orange dye solution mixed with $Zn0._{999900}Gd_{0.000100}O$ Fig. 6b. These results clearly show that aqueous methyl orange solution was degraded by the addition of $Zn_{1-x}Gd_xO$ nanophotocatalyst. Fig. 7a and b represents the plots of dye concentration versus the UV irradiation time (t) and plots of $\ln(C_0/C_t)$ versus the UV irradiation time (t) respectively for pure and Gd-doped ZnO nanopowders. Plots of $\ln(C_0/C_t)$ versus the UV irradiation time (t) suggest that the photodegradation of methyl orange dye follows the pseudo-first order kinetics. The values of first-order rate constants (k)

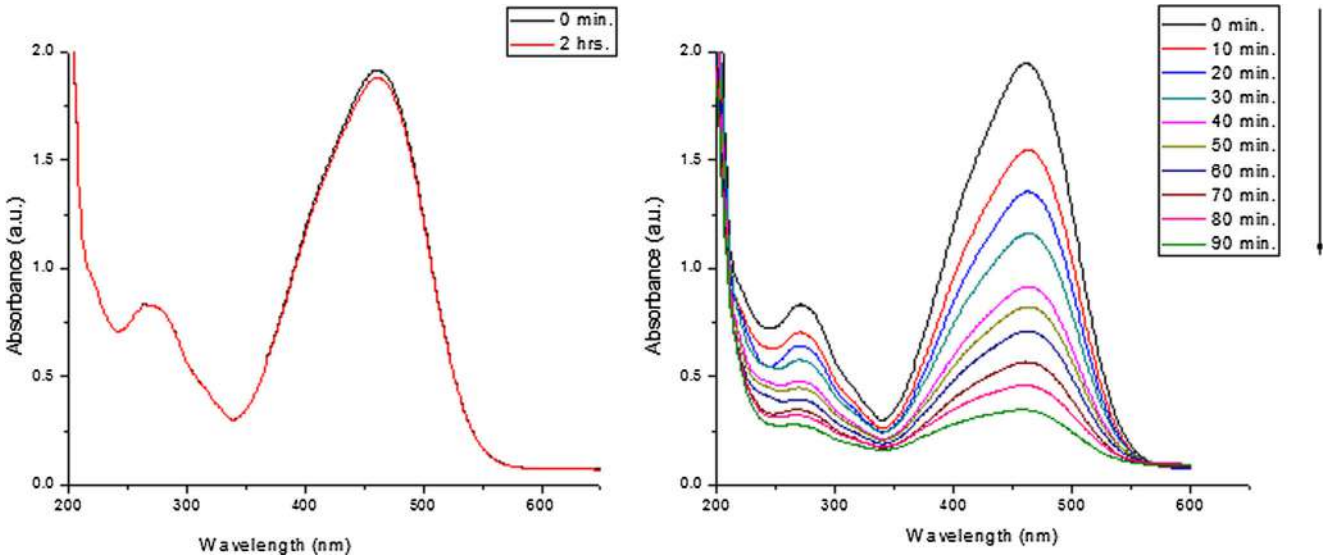

Fig. 6. Ultraviolet–visible spectra of the methyl orange dye in aqueous solution upon irradiation with ultraviolet light in the (a) absence of photocatalyst (b) presence of $Zn_{0.9999}Gd_{0.0001}O$ nanocrystals. (For interpretation of the references to colour in this figure legend, the reader is referred to the web version of this article.)

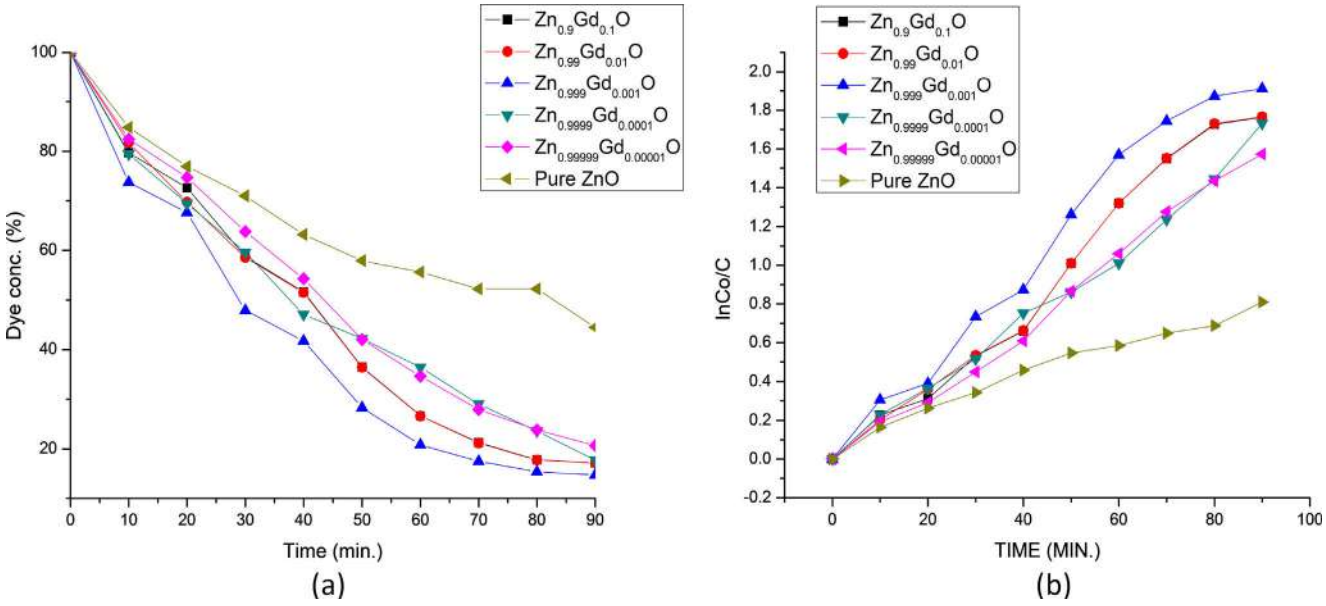

Fig. 7. (a) plots of dye concentration versus the UV irradiation time (t) (b) plots of ln(C0/Ct) versus the UV irradiation time (t).

are 1.96 × 10^{-2} min^{-1}, 1.96 × 10^{-2} min^{-1}, 2.12 × 10^{-2} min^{-1}, 1.92 × 10^{-2} min^{-1}, 1.75 × 10^{-2} min^{-1} and 0.9 × 10^{-2} min^{-1} where as the degradation efficiency (ε) values are 82.83%, 82.89%, 85.30%, 82.30%, 79.33% and 55.50% for various $Zn_{1-x}Gd_xO$ nanoparticles with × = 0.10000, 0.01000, 0.00100, 0.00010, 0.00001 and 0.00000, respectively. The photocatalytic performance is directly proportional to the value of apparent rate constants (k) calculated from the linear fitted curves using Eq. (4). After comparing the values of k, it can be stated that the doping of ZnO with gadolinium has significantly increased its photocatalytic efficiency. Among various doped Zn O nanomaterials, the increasing order The maximum increase is noted in case of $Zn_{0.99900}Gd_{0.00100}O$ nanocrystals (ε = 85.3% and k = 2.12 × 10^{-2} min^{-1}) whereas it is minimum in case of $Zn0._{99999}Gd_{0.00001}O$ nanocrystals (ε = 79.3% and k = 1.75 × 10^{-2} min^{-1}).

Photocatalytic degradation scheme of MO dye under UV light irradiation in the presence of Gd-doped ZnO nanoparticles occurs by following proposed mechanism:

Step I: Absorption of light by Gd doped ZnO nanoparticles that excite electron from valence band to conduction band thus creating a positive hole in valence band.

Step II: Positive holes react with hydroxyl ions produced by ionization of chemisorbed water molecules to produce $O\dot{H}$ radicals, whereas electrons in conduction band reduce oxygen to form superoxide radical $\dot{O_2}$.

Step III: $O\dot{H}$ radicals, being strong oxidizing agents, react with organic dye molecules to cause their complete degradation. The complete mineralization of MO molecule is indicated by decolorization of its intense orange colored aqueous solution and it undergoes demethylation, oxidation and hydroxylation process results in the formation of inorganic products such as SO_4^{2-} ions, NO_3^- ions, CO_2 and H_2O.

The photocatalytic activity of photocatalysts largely depends upon the reducing tendency of electron hole recombination. Presence of various intrinsic and extrinsic defects in such compounds has significantly increased the separation time for electron hole recombination. Intrinsic defects namely oxygen vacancies are the characteristic features of ZnO nanoparticles. Talking about extrinsic defects, doping of ZnO with Gd allows entry of Gd^{3+} into the crystal lattice of ZnO thus creating Zn^{2+} vacancy defects. These extrinsic and intrinsic defects in Gd doped ZnO nanostructures together retard the electron hole recombination time and inturn the photocatalytic efficiency of nanoparticles towards the degradation of methyl orange dye has increased.

4. Conclusions

Bottom up Chemical co-precipitation technique has been successfully employed for the synthesis of pure and Gd-doped ZnO nanoparticles. The insertion of Gd into ZnO has been confirmed from EDXRF studies, while the nanosize wurtzite structure has been revealed from XRD studies. Photocatalytic degradation of methyl orange dye has studied under UV irradiation in the presence of prepared nanoparticles. It suggests that the catalytic efficiency of ZnO photocatalyst have enhanced upon doping with Gadolinium.

Credit author statement

It is a single author paper. All the work is done by author alone.

Declaration of Competing Interest

The authors declare that they have no known competing financial interests or personal relationships that could have appeared to influence the work reported in this paper.

Acknowledgements

I am thankful to the UGC, New Delhi, India, for financial support under College for Potential and Excellence research grant. I acknowledge the guidance and support provided by Dr. Dharminder Singh Ubha, Principal, G.S.S.D.G.S. Khalsa College, Patiala. I am also thankful to Dr. Narinder Singh, Associate Professor, I.I.T., Ropar, Punjab for using his laboratory facilities.

References

[1] M.A. Rauf, I. Shehadeh, A. Ahmed, A. Al-Zamly, J. Int. Chem., Mol. Nuc. Mater. Metallurg. Eng. 3 (7) (2009) 369–374.
[2] M. Catanho, G.R.P. Malpass, A.J. Motheo, Quimica Nova 29 (2006) 983–989.
[3] M. Faisal, M.A. Tariq, M. Muneer, Dyes Pigm 72 (2007) 233–239.
[4] R.J. Kant, Nat Sci. 4 (2012) 22–26.
[5] T. Zhang, T. Oyama, S. Horikoshi, H. Hidaka, J. Zhao, N. Serpone, Solar Ener. Mater. Solar Cells 73 (3) (2002) 287–303.
[6] Sobczyński, A., and Dobosz, A. Polish J. Environ. Studies, 2001, 10(4), 195–205.
[7] T.M. Elmorsi, Y.M. Riyad, Z.H. Mohamed, H.M.H. Abid, E. Bary, J. Hazard. Mater. 174 (2010) 352–356.
[8] S. Gul, O. Ozcan Yildlrln, Chem. Eng. J. 155 (2009) 684–690.
[9] F.H. AlHamedi, M.A. Rauf, S.S. Asraf, Desalination 239 (2009) 159–166.
[10] R. Wahab, S.K. Tripathy, H.S. Shin, M. Mohapatra, J. Musarrat, A.A.A. Khedhairy, N.K. Kaushik, Chem. Eng. J. 226 (2013) 154–160.
[11] S.K. Kansal, A.H. Ali, S. Kapoor, Desalination 259 (1–3) (2010) 147–155.

[12] A. Kajbafvala, H. Ghorbani, A. Paravar, J.P. Samberg, E. Kajbafvala, S.K. Sadrnezhaad, Superlattice Microst. 51 (4) (2012) 512–522.
[13] P.K. Chen, G.J. Lee, S.H. Davies, S.J. Masten, R. Amutha, J.J. Wu, Mater. Res. Bull. 48 (6) (2013) 2375–2382.
[14] L. Xu, Z. Li, Q. Cai, H. Wang, H. Gao, W. Lv, J. Liu, Cryst. Eng. Comm. 12 (2010) 2166–2172.
[15] A. Senthilraja, B. Subash, B. Krishnakumar, D. Rajamanickam, M. Swami-nathan, M. Shanthi, Mater. Sci. Semicond. Process. 22 (2014) 83–91.
[16] H. Wu, W. Pan, J. Am. Ceram. Soc 89 (2006) 699–701.
[17] C.A.K. Gouvea, F. Wypych, S.G. Moraes, N. Duran, P. Peralta-Zamor, Chemosphere 40 (4) (2000) 427–432.
[18] N. Elamin, A. Elsanousi, J. App. Indust. Sci. 1 (2013) 32–35.
[19] Q. Xiao, L.J. Ouyang, Alloy. Compd. 479 (1–2) (2009) 4–7.
[20] J. Zhi-gang, P. Kuan-kuan, L.I. Yan-hua, Z. Rongsun, Trans. Nonferrous Met. Soc. China 12 (2012) 873–878.
[21] S. Ekambaram, Y. Iikubo, A.J. Kudo, Alloy. Compd. 433 (1–2) (2007) 237–240.
[22] F. Min, Y. Li, W. Siwei, L. Peng, J. Liu, F. Dong, Appl. Surf. Sci. 258 (4) (2011) 1587–1591.
[23] M.M.B. Abbad, A.A.H. Kadhum, A.B. Mohamad, M.S. Takriff, K. Sopian, Chemosphere 91 (11) (2013) 1604–1611.
[24] V. Vaiano, M. Matarangolo, O. Sacco, D. Sannino, Chem. Eng. Trans. 57 (2017) 625–630.
[25] U. Alam, A. Khan, D. Ali, D. Bahnemann, M. Muneer, RSC Adv. 8 (2018) 17582–17594.
[26] C. Jun-Lian, D. Neena, L. Na, F. De-Jun, K. Xian-Wen, Chin. Phys. B 27 (8) (2018) 086102.
[27] Hu, B., Sun, Q., Zuo, C., Pei, Y., Yang, S., Zheng, H., Liu, F. Beilstein J. Nanotechnol., 2019, 10, 1157–1165.
[28] H. Parangusan, D. Ponnamma, M.A.A. Al-maadeed, Bull. Mater. Sci. 42 (2019) 179.
[29] A. Samanta, M.N. Goswami, P.K. Mahapatra, Mater. Res. Express 6 (2019) 065031.
[30] P. Pascariu, C. Cojocaru, N. Olaru, P. Samoila, A. Airinei, M. Ignat, L. Sacarescu, D.J. Timpu, Environ. Manage. 239 (2019) 225–234.
[31] K.J. Laidler, J.H. Meiser, ISBN 0-8053-5682-7, Phys. Chem. (1982) 780.
[32] Joint Committee on Powder Diffraction Standards (JCPDS) File No. 05-0664.
[33] V. Rajendar, T. Dayakar, K. Shobhan, I. Srikanth, K.V. Rao, Superlatt. Microstruc. 75 (2014) 551–563.
[34] C.N.R. Rao, Chemical Applications of Infrared spectroscopy, Academic Press, New York and London, 1963.
[35] M.I.H. Chowdhury, M.S. Hossain, M.A.S. Azad, M.Z. Islam, M.A. Dewan, IJSER 9 (6) (2018) 1646–1649.
[36] X. Chen, Z. Wu, D. Liu, Z. Gao, Nanoscale Res Lett 12 (2017) 143.
[37] L.A. Ghule, A.A. Patil, K.B. Sapnar, S.D. Dhole, K.M. Garadkar, Toxicol. Environ. Chem. 93 (4) (2011) 623–634.
[38] T.R. Giraldi, G.V.F. Santos, V.R. Mendonça, C. Ribeiro, I.T. Weber, J. Nanosci. Nanotechnol. 11 (4) (2011) 43635–43640.